Cell, Volume *134*

Supplemental Data

HIV Envelope-CXCR4 Signaling Activates Cofilin to Overcome Cortical Actin Restriction in Resting CD4 T Cells

Alyson Yoder, Dongyang Yu, Li Dong, Subashini R. Iyer, Xuehua Xu, Jeremy Kelly, Juan Liu, Weifeng Wang, Paul J. Vorster, Liane Agulto, David A. Stephany, James N. Cooper, Jon W. Marsh, and Yuntao Wu

Table of Contents

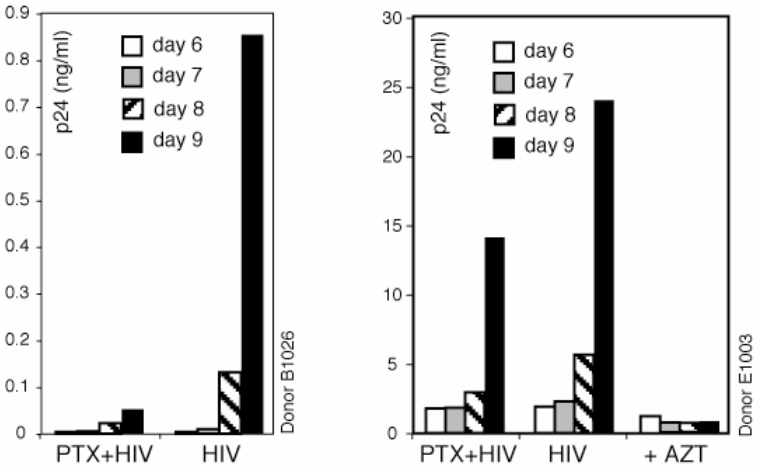

Figure S1. Inhibition of HIV-1 infection of resting CD4 T cells by pertussis toxin

Resting CD4 T cells from two additional donors were treated with pertussis toxin (PTX) (100 ng/ml) or untreated for 2 hours, infected with HIV for 2 hours, washed, cultured for 5 days, and then activated with anti-CD3/CD28 magnetic beads (four beads per cell) at day 5. Shown is viral replication measured by p24 release from day 6 to 9 post infection. As a control, in one donor, cells were also treated with AZT (50 μM) for 12 hours before infection, and then infected with HIV, washed, cultured in the continuous presence of AZT. AZT completely inhibited viral replication.

PTX inhibition of HIV-1 infection of resting CD4 T cells has also been observed in 15 other donors (data not shown)

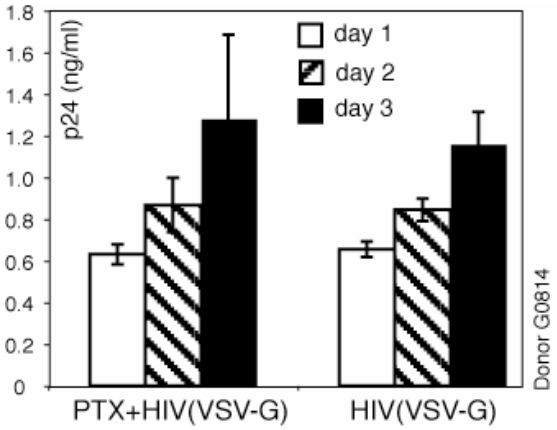

Figure S2. Pertussis toxin does not inhibit VSV-G pseudo-typed HIV-1 infection of resting CD4 T cells

VSV-G envelope mediates HIV-1 entry through endocytosis, which does not involve binding to CXCR4 receptor. To determine whether VSV-G pseudo-typed HIV-1 requires G protein signaling, HIV-$1_{(KFS)}$ (Freed et al., 1992) pseudotyped with VSV-G was used for infection of resting CD4 T cells. Cells were treated with PTX (100 ng/ml) or medium for 2 hours and then infected with HIV-1(VSV-G) (0.35 $TCID_{50/Rev\text{-}CEM}$ per cell) for 2 hours. Following infection, cells were washed three times and resuspended into fresh medium. Because VSV-G pseudo-typed HIV-1 has a half life of only 1 day in resting CD4 T cells (Pierson et al., 2002), infected cells were activated at day 1 post infection and viral replication was monitored for three days. Shown is p24 release following activation.

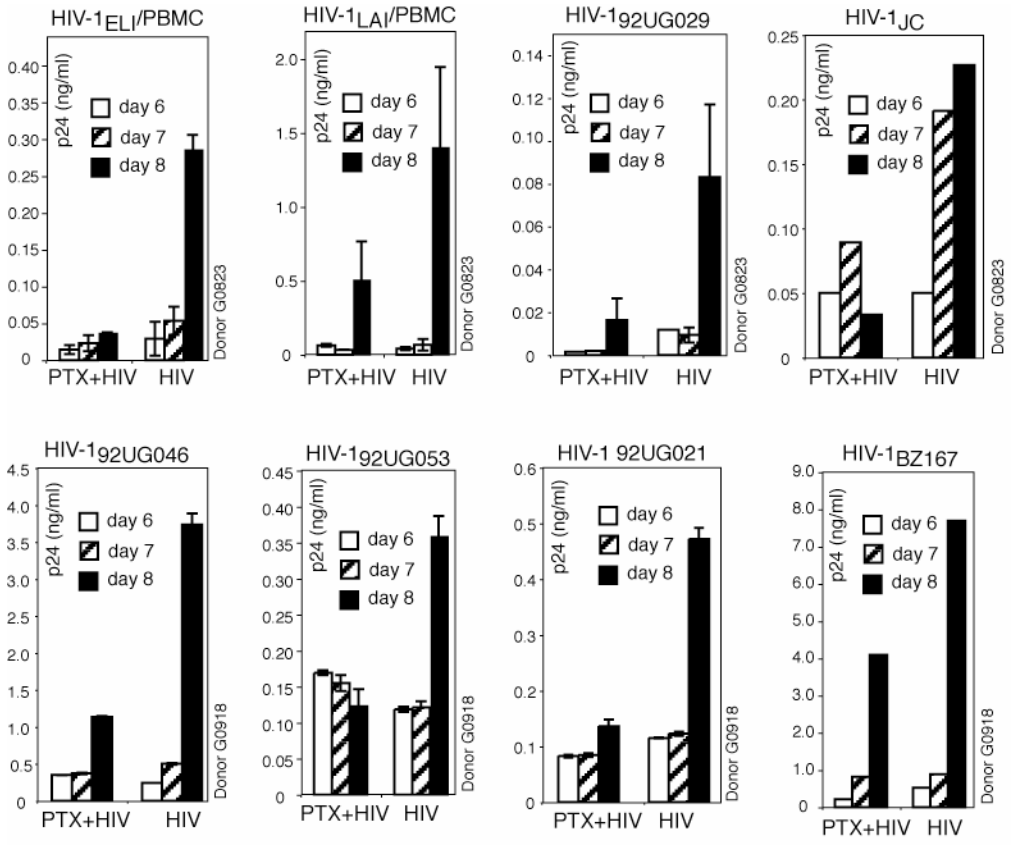

Figure S3. Pertussis toxin inhibits infection of resting CD4 T cells by multiple primary isolates of HIV-1

Eight primary HIV-1 isolates (provided by the NIH AIDS Research & Reference Reagent Program) were used to infect resting CD4 T cells in the presence or absence of PTX (100 ng/ml). Resting CD4 T cells from two donors were purified, treated with PTX for 2 hours, infected with HIV-1 for 2 hours, washed, cultured for 5 days, and then activated with anti-CD3/CD28 magnetic beads (4 beads per cell) at day 5. Shown is viral replication measured by p24 release from day 6 to 8 post infection. Viral dosages used for infection of $1x10^6$ cells: HIV-$1_{ELI/PBMC}$($10^{4.5}TCID_{50}$), HIV-$1_{LAI/PBMC}$ ($10^{4.5}TCID_{50}$), HIV-1_{JC}($10^{3.2}TCID_{50}$), HIV-$1_{92UG046}$($10^{4.8}TCID_{50}$), HIV-$1_{92UG053}$($10^{4.0}TCID_{50}$), HIV-$1_{92UG021}$($10^{4.6}TCID_{50}$), HIV-1_{BZ167}($10^{5.1}TCID_{50}$).

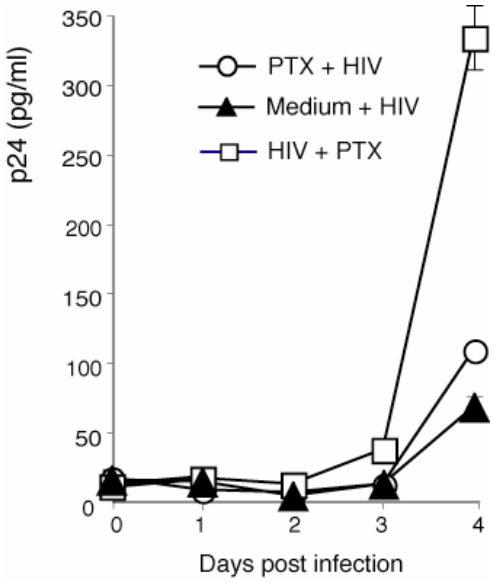

Figure S4. Inhibition of CXCR4 signaling by PTX does not inhibit viral replication in transformed T cell lines

CEM-SS cells were treated with PTX (100 ng/ml) or medium for 2 hours, and then infected with HIV-1 for 2 hours. Following infection, cells were washed three times and resuspended into fresh medium. Cells were also infected with HIV-1 first, washed once, treated with PTX for 4 hours, washed again, and resuspended into fresh medium. Shown is p24 release following infection.

Note: Chemokine receptor signaling has been shown to be unnecessary for HIV infection of transformed cell lines . However, we observed that PTX inhibited HIV infection of resting CD4 T cells (Figure 1A). To determine whether PTX inhibits viral replication in transformed T cell lines, we briefly treated a human T cell line, CEM-SS, with PTX and then infected them with HIV-1. The treatment and infection were identical to those of resting CD4 T cells (Figure 1A). We monitored viral replication following infection and observed no inhibition of viral replication by PTX (Figure S4), confirming the previous conclusions that CXCR4 signaling does not appear to be required for HIV-1 infection of transformed T cell lines. Similar results were also observed with PHA plus IL-2-activated CD4 T cells (data not shown). Thus, inhibition of viral replication by PTX is unique to HIV infection of resting CD4 T cells.

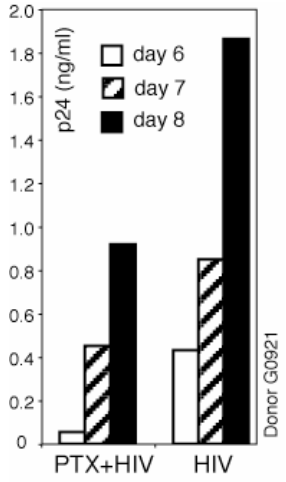

Figure S5. Pertussis toxin inhibits HIV-1 infection of tonsillar resting CD4 T cells

Resting CD4 T cells were purified from tonsillar tissue cell suspension by two rounds of negative depletion, using the same method as the isolation of resting CD4 T cells from the peripheral blood described in the Supplemental Methods. Cells were directly treated with PTX for 1 hour, infected with HIV-1 (0.02 $TCID_{50/Rev\text{-}CEM}$ per cell) for 2 hours, washed, cultured for 5 days, and then activated with anti-CD3/CD28 magnetic beads. Shown is viral replication measured by p24 release from day 6 to 8 post infection. PTX inhibition of HIV-1 infection of tonsillar CD4 T cells was also observed in another donor (data not shown).

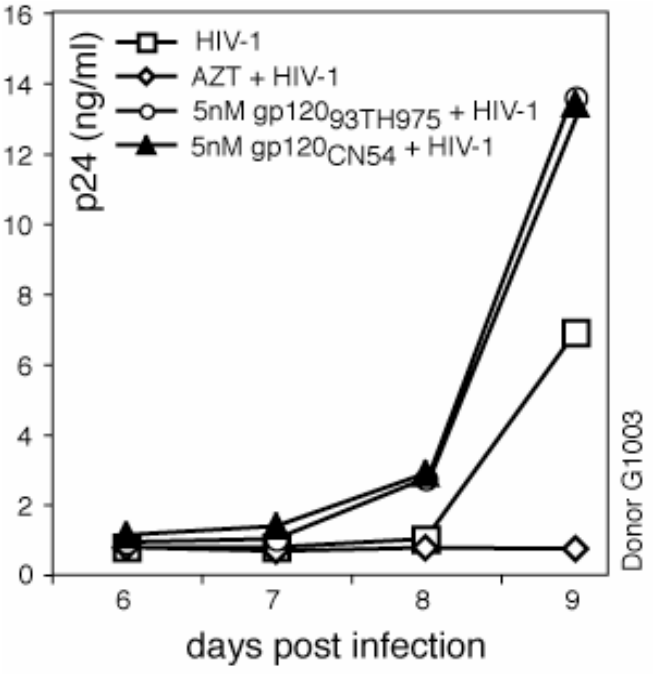

Figure S6. Enhancement of HIV-1 infection of resting CD4 T cells by gp120 stimulation

Resting CD4 T cells were stimulated with 5 nM of $gp120_{93TH975}$ or 5 nM $gp120_{CN54}$ for overnight, then infected with HIV (0.02 $TCID_{50/Rev\text{-}CEM}$ per cell) for 2 hours. Following infection, cells were washed and continuously incubated with 5 nM gp120 for 5 days, and then activated with anti-CD3/CD28 beads (4 beads per cell). Shown is viral replication measured by p24 release. As a control, 50 μM AZT was used and added 12 hours before infection and remained in the culture during the whole replication course.

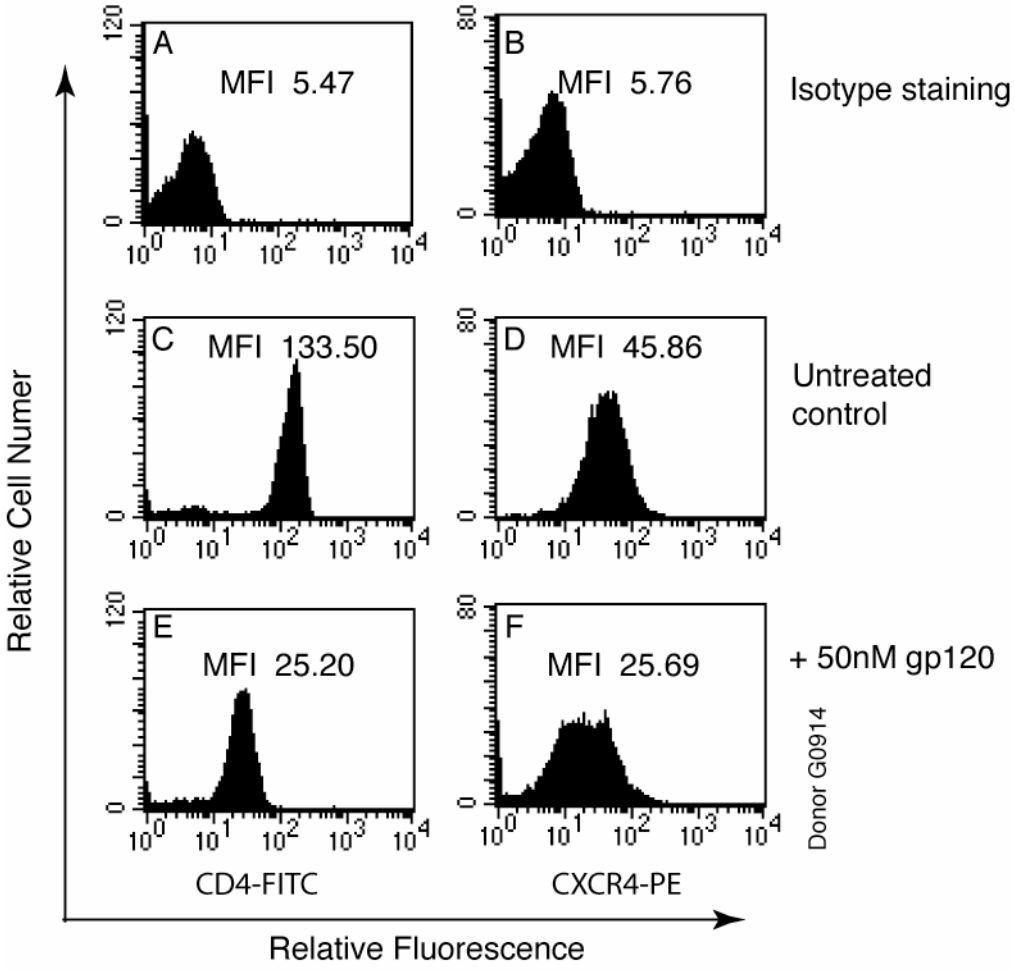

Figure S7. Down-modulation of CD4, CXCR4 receptor on resting CD4 T cells by 50nM gp120

Resting CD4 T cells were not treated (C, D) or treated with 50 nM gp120 for 1 hour (E, F), then washed with PBS plus 0.1% BSA and stained with monoclonal antibodies against CD4 or CXCR4 labeled with FITC or PE. The mean fluorescent intensity (MFI) of staining is shown. Isotype control staining is shown in A and B.

Our data are consistent with previous demonstration of down-modulation of CD4 and CXCR4 by gp120 (Su et al., 1999).

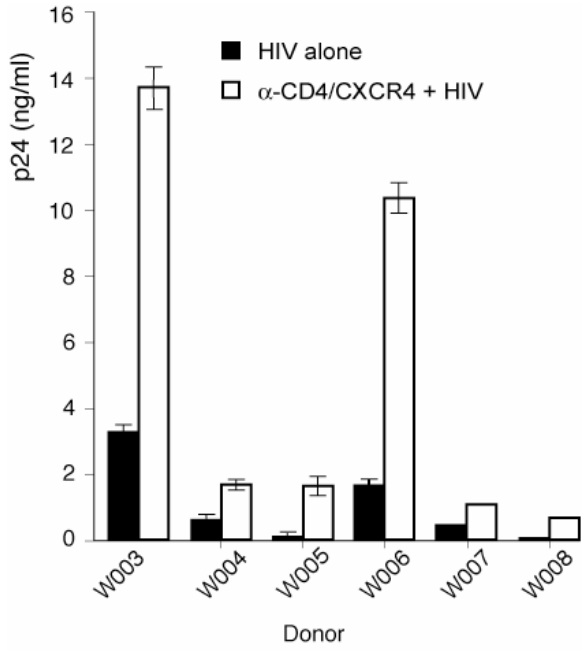

Figure S8. Enhancement of HIV-1 latent infection of resting CD4 T cells by anti-CD4/CXCR4 magnetic beads in multiple donors

Resting CD4 T cells were pre-stimulated overnight with magnetic beads coated with antibodies against CD4/CXCR4 at 2 beads per cell, and then infected with HIV-1. Cells were incubated for 5 days and activated by anti-CD3/CD28 magnetic beads (2 beads per cell). Shown is viral replication at day 8.

Note: We used magnetic beads conjugated with monoclonal antibodies to stimulate CD4 and CXCR4, and observed enhancement of HIV-1 infection (Figure 1J). The experiment was reproduced in multiple donors to determine whether the enhancement was donor dependent. We tested six additional donors and observed the enhancement in every donor tested (Figure S8). The average enhancement was 7.5 fold, although the extent of enhancement varied among donors from 2 to 17 fold.

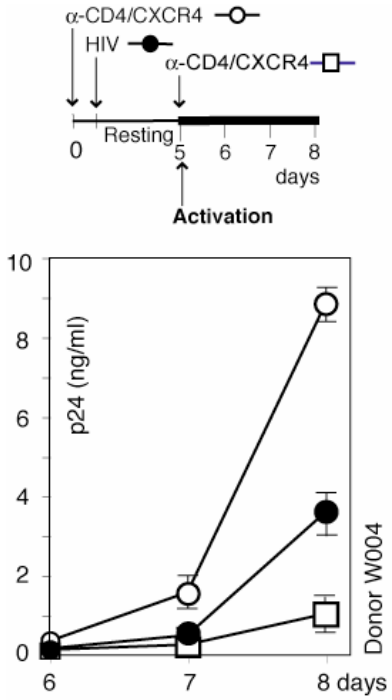

Figure S9. Enhancement of viral replication by Anti-CD4/CXCR4 beads does not result from synergistic enhancement of T cell activity

Resting CD4 T cells were stimulated with anti-CD4/CXCR4 beads (2 beads per cell) either prior to infection (open circle) or after infection (square) at day 5 during T cell activation with anti-CD3/CD28 beads (2 beads per cell). As a control, CD4/CXCR4-unstimulated T cells were identically infected and activated (closed circle). Shown is viral replication from day 6 to 8. Viral replication was enhanced with anti-CD4/CXCR4 beads added prior to infection, whereas viral replication was inhibited with anti-CD4/CXCR4 beads added at the time of T cell activation, suggesting that the enhancement by anti-CD4/CXCR4 beads is unlikely the results of synergy between CD4/CXCR4 stimulation and CD3/CD28 stimulation.

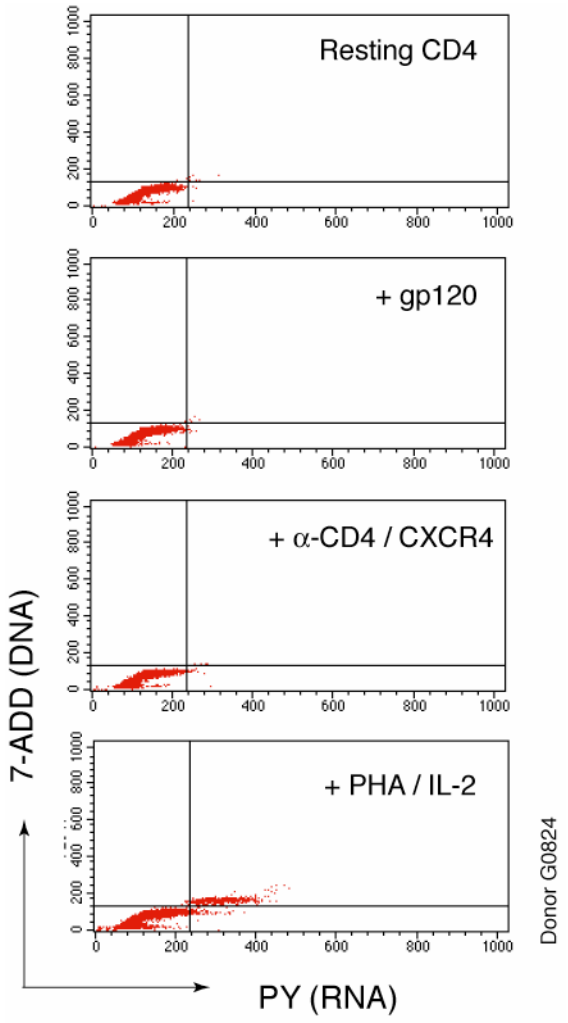

Figure S10. Lack of cell cycle progression in resting T cells pre-stimulated with gp120 or anti-CD4/CXCR4 beads

Cells were incubated with gp120IIIB (50 nM) or anti-CD4/CXCR4 BD IMag particles for 5 days, and then analyzed for cell cycle progression using 7-AAD, PY staining as described in Supplemental Methods. PHA plus IL-2-stimulated cells were used as a control.

Note: To determine whether the enhancement of viral latent infection by gp120 or anti-CD4/CXCR4 beads resulted from activation of resting CD4 T cells, we carried out a cell cycle analysis of resting CD4 T cells treated with gp120 or anti-CD4/CXCR4 beads for 5 days. As shown in Figure S10, we observed no cell cycle progression induced by these stimuli. In contrast, PHA plus IL-2 stimulated T cells into the cell cycle.

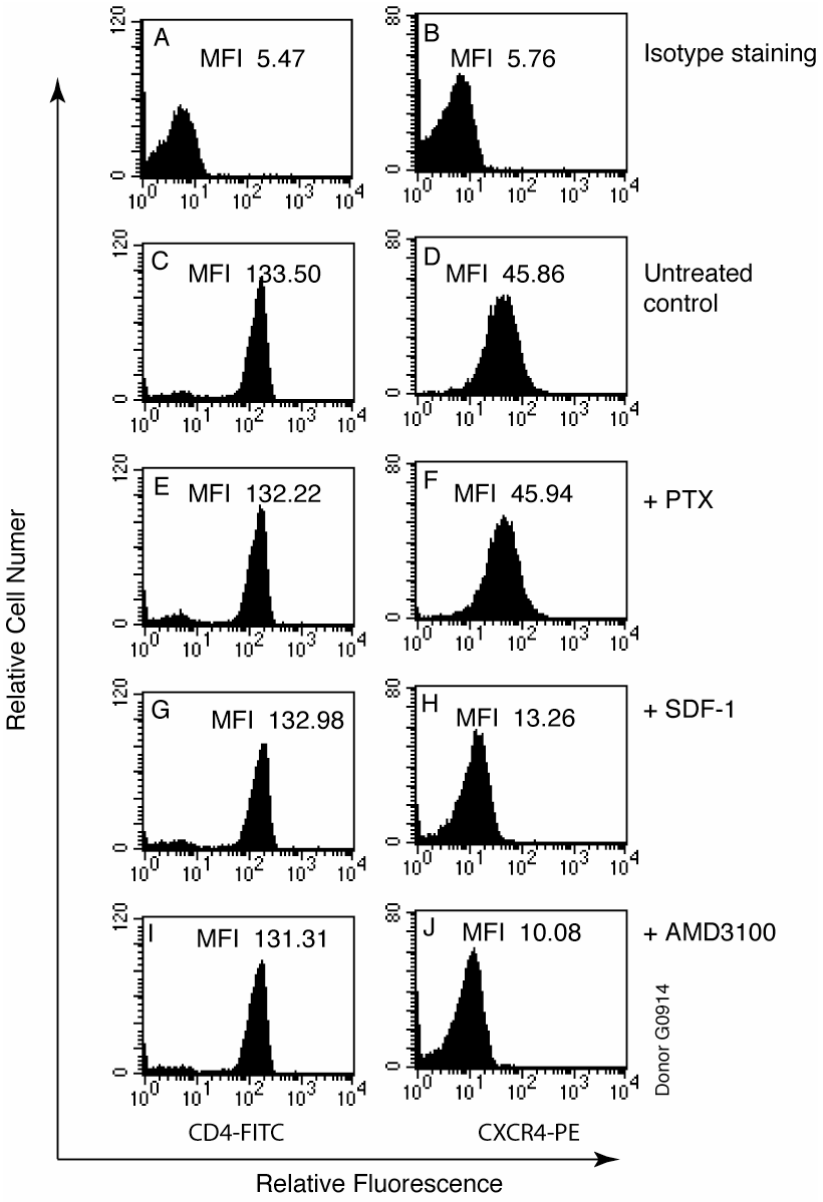

Figure S11. PTX treatment of resting CD4 T cells does not down-modulate CD4 or CXCR4 receptor

Resting CD4 T cells were not treated (C, D) or treated with PTX (100 ng/ml) for two hours (E, F), washed, and then stained with a FITC-labeled anti-human CD4 antibody (C, E) or a PE-labeled anti-human CXCR4 antibody (D, F). Staining with the Isotype antibodies is shown in A and B, respectively. As controls, cells were also treated with the CXCR4 ligand, SDF-1 (2 μg/ml) or a CXCR4 antagonist, AMD3100 (1 μg/ml), for 1 hour, washed and then similarly stained. Both SDF-1 and AMD3100 down-modulate the CXCR4 receptor (H, J), while leave the CD4 receptor unaffected (G, I). Changes in the mean fluorescent intensity (MFI) after various treatments are shown.

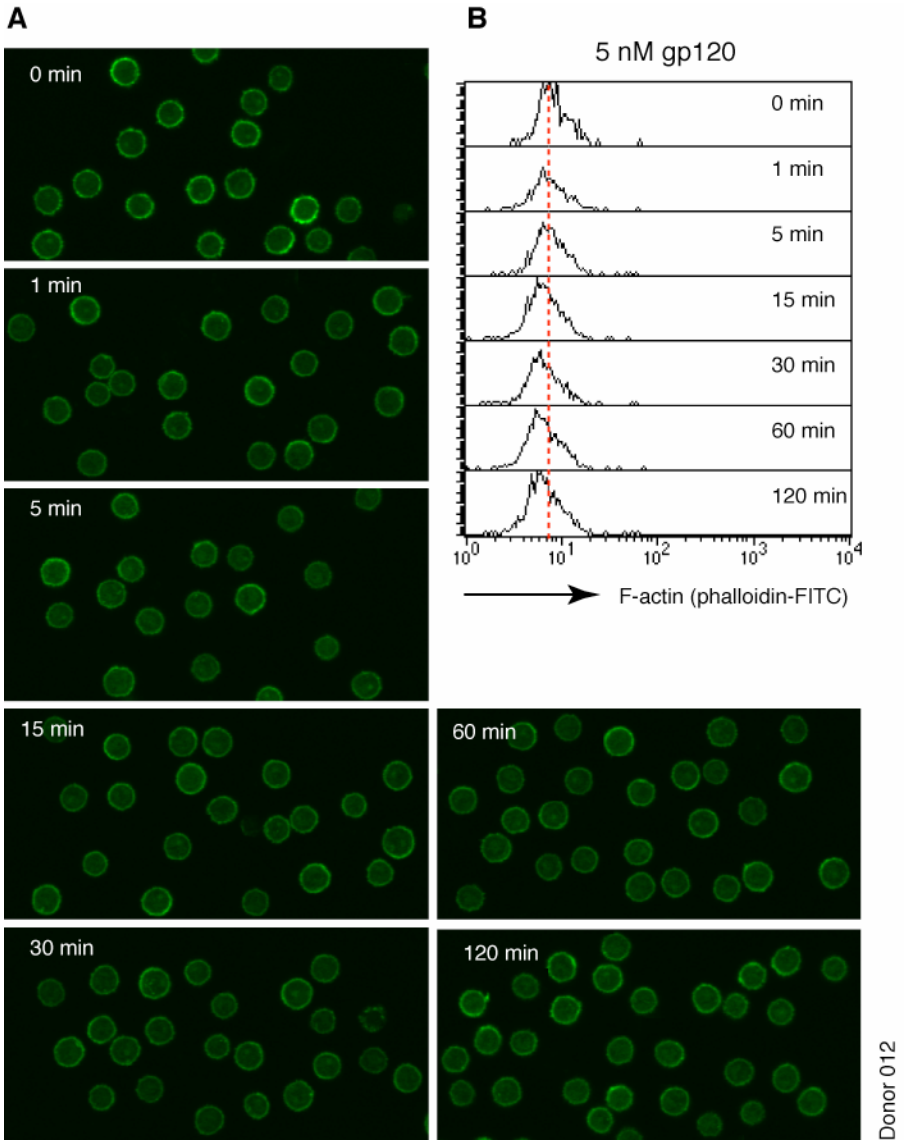

Figure S12. Actin dynamics mediated by HIV-1 envelope binding to resting CD4 T cells

To confirm the conclusion that HIV-1 gp120 binding to CXCR4 promotes actin dynamics in resting CD4 T cells, cells from additional donors were treated with 5 nM gp120 IIIB. Treated cells were taken at various time points and stained with FITC-Phalloidin as described in Supplemental Methods. F-actin staining was visualized by confocal microscopy (A) (images were acquired under identical conditions and cells were randomly selected), and quantified by flow cytometry (B). In this particular donor, gp120 binding triggered depolymerization of cortical actin after 15 minutes. Similar actin depolymerization was also observed with 5 pM gp120 (data not shown)

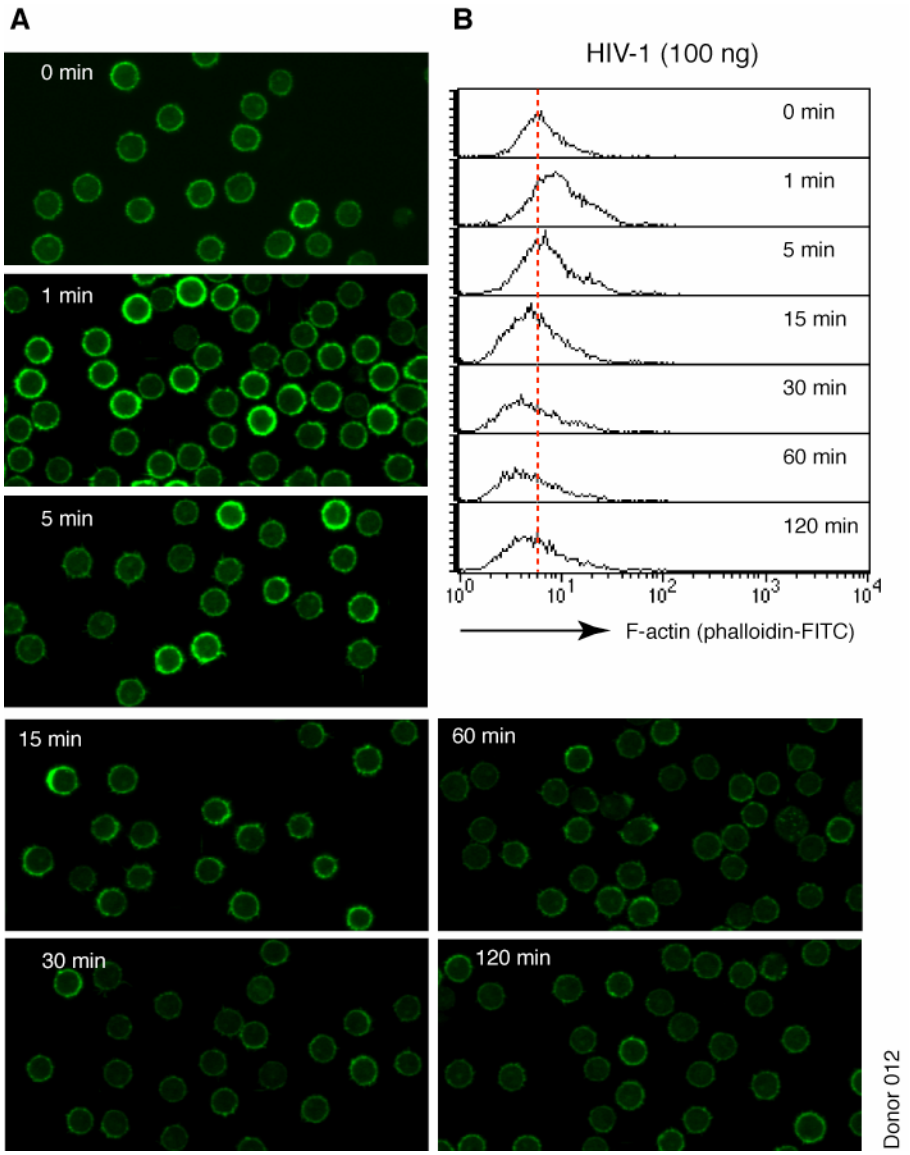

Figure S13. Actin dynamics mediated by HIV-1 particle binding to resting CD4 T cells

To confirm the conclusion that HIV-1 binding to CXCR4 promotes actin dynamics in resting CD4 T cells, cells from additional donors were treated with 100 ng (p24) of HIV-1_{NL4-3}. Cells were taken at various time points and stained with FITC-Phalloidin as described in Supplemental Methods. F-actin staining was visualized by confocal microscopy (A) and quantified by flow cytometry (B). In this particular donor, HIV-1 binding triggered a quick cortical actin polymerization at 1 minute, followed by depolymerization after 5 minutes.

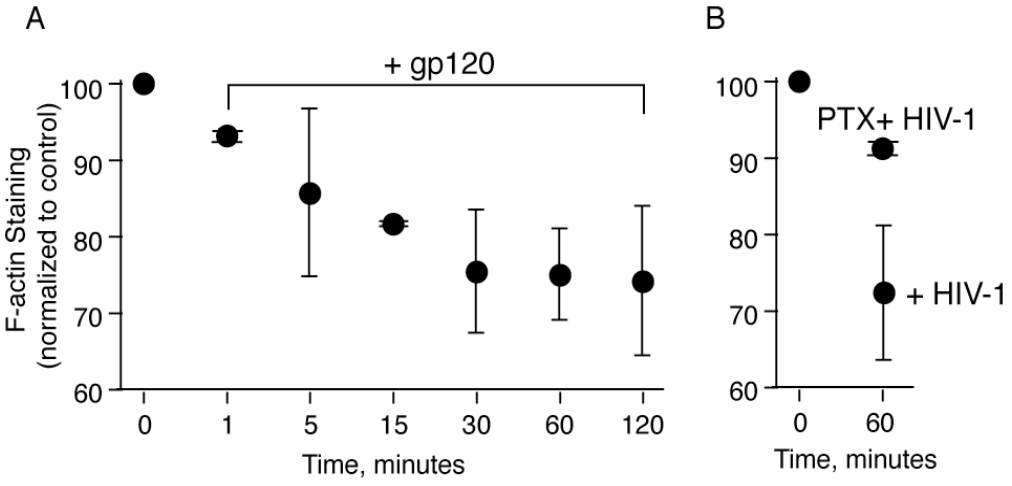

Figure S14. Quantification and statistic analysis of F-actin staining following gp120 and HIV-1 exposure

(A) Cells from three donors were treated with 5 nM gp120 IIIB for the defined times, fixed, stained with FITC-Phalloidin and then analyzed by flow cytometry as described in Supplemental Methods. The geometric mean fluorescence of untreated populations was set to 100% F-actin staining and all experimental data for that particular donor were normalized to that value of fluorescence. Graphed data points represent the mean ± standard error (n=3). Similar analysis was also applied to additionally three donors treated with HIV-1 or PTX plus HIV-1 (B). Only the 0 and 60 minute samples are shown.

For comparison of the F-actin staining in Figures 3 and S12 to S14, statistical analyses by the Kolmogorov-Smirnov two sample test (Young, 1977) were used to determine if there was a significant change (loss) in F-actin staining of the 60 minute-treated population compared to the untreated control population (from the same donor), where treatment was exposure to either 5 nM gp120 (3 donors) or 100 ng p24 HIV-1 (4 donors), as described in Supplemental Methods. The D and D/s(n) statistics (given as D;D/s(n)) for the gp120 experiments were 0.35;6.18, 0.25;22.27, and 0.49;27.65. The analyses for 100 ng HIV experiments: 0.34;20.32, 0.42;37.14, 0.15;13.23, 0.30;13.15. For all 7 analyses, the loss of F-actin staining of the experimental populations was found to be significantly different from that of the untreated control cell populations from the same donor ($P <= 0.001$ for all analyses). Analysis of flow cytometric data was accomplished with Cell Quest software (BD Biosciences) and Prism software (GraphPad).

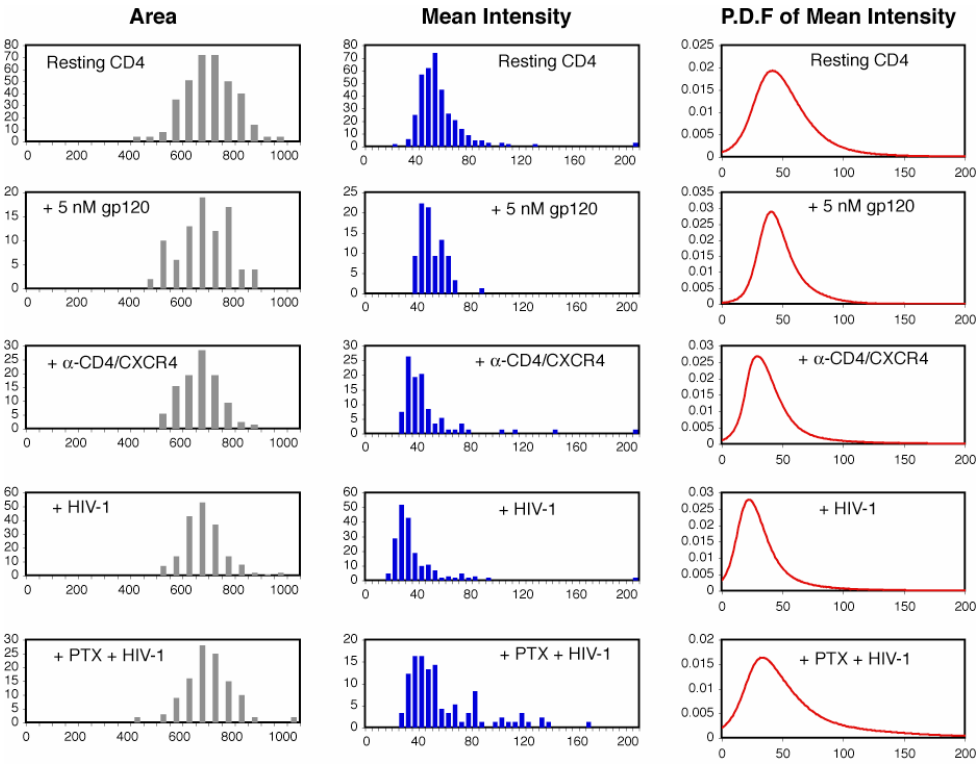

Figure S15. Quantification of confocal images of cortical actin in resting CD4 T cells

For quantification of confocal images in Figure 3E, S12 and S13, T cells (untreated or treated with gp120, CD4/CXCR4-particles, HIV-1, PTX plus HIV-1 for 2 hours) were automatically detected using a customized Matlab (Mathworks, Inc.) script (http://www.tobScope.com). Changes in the staining intensity were selected by edge detection, and the binary edge detection mask was then dilated and smoothed to yield an outline for each cell. Fluorescent intensities were determined per cell by calculating the values for pixels within each outline.

The "area" plots in the left column represent the distribution of cell size selected for analyses. The x-axis is the relative size of the cell, whereas the y-axis is the count of cells. The "mean intensity" plots in the middle column show the histogram (cell number in y-axis) of the mean fluorescence intensities (in pixels) per cell (x-axis). The "P.D.F" plots in the right column represent "Probability Density Function", which calculates the possibility (y-axis) of each fluorescent intensity (x-axis). The total area under the red curve line is defined as "1". The number of cells used for each analysis:
Untreated resting CD4 T cells = 346
gp120 treated resting CD4 T cells = 87
CD4/CXCR4 particle treated resting CD4 T cells = 98
HIV-1 treated resting CD4 T cells = 181
PTX plus HIV-1 treated resting CD4 T cells = 112

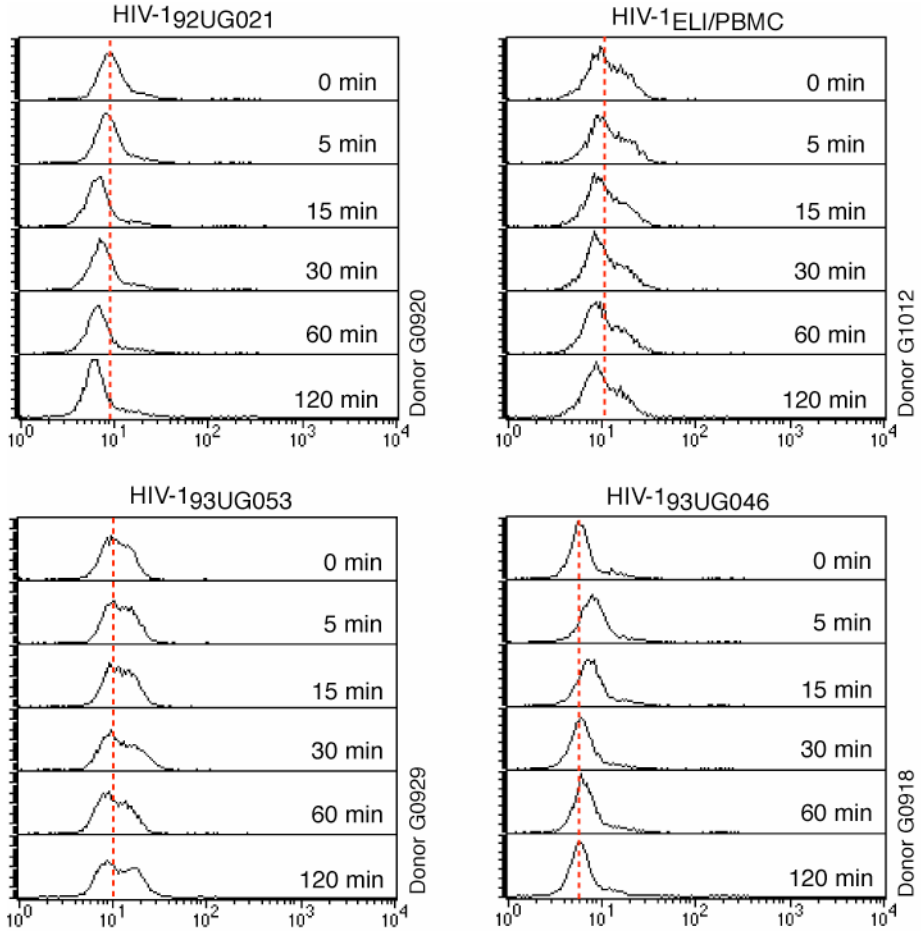

Figure S16. F-actin changes mediated by multiple primary isolates of HIV-1 and gp120

To confirm that the ability of HIV-1 gp120 to trigger actin dynamics was not limited to only laboratory-adapted strains, resting CD4 T cells were treated with HIV-$1_{92UG021}$, HIV-$1_{ELI/PBMC}$, HIV-$1_{92UG053}$, HIV-$1_{92UG046}$ (2-50 ng p24 per million cells). Cells were treated for various times, fixed, permeabilized, stained with FITC-phalloidin, and then analyzed by flow cytometry.

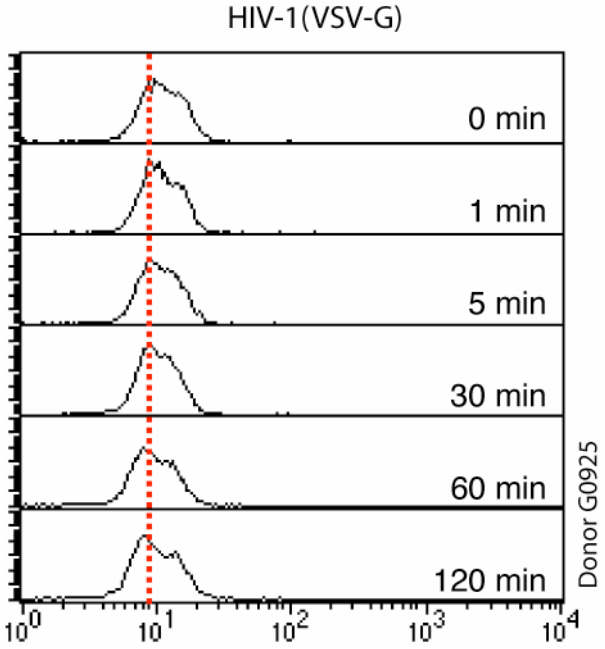

Figure S17. VSV-G envelope does not mediate F-actin change in resting CD4 T cells

VSV-G envelope mediates HIV-1 entry through endocytosis, which does not involve binding of CXCR4 receptor. To determine whether VSV-G envelope can trigger any actin change in resting T cells, HIV-$1_{(KFS)}$ was pseudo-typed with VSV-G envelope and then used to treat resting CD4 T cells (100 ng per million cells) for various times. Cells were fixed, permeabilized, stained with FITC-phalloidin, and then analyzed by flow cytometry.

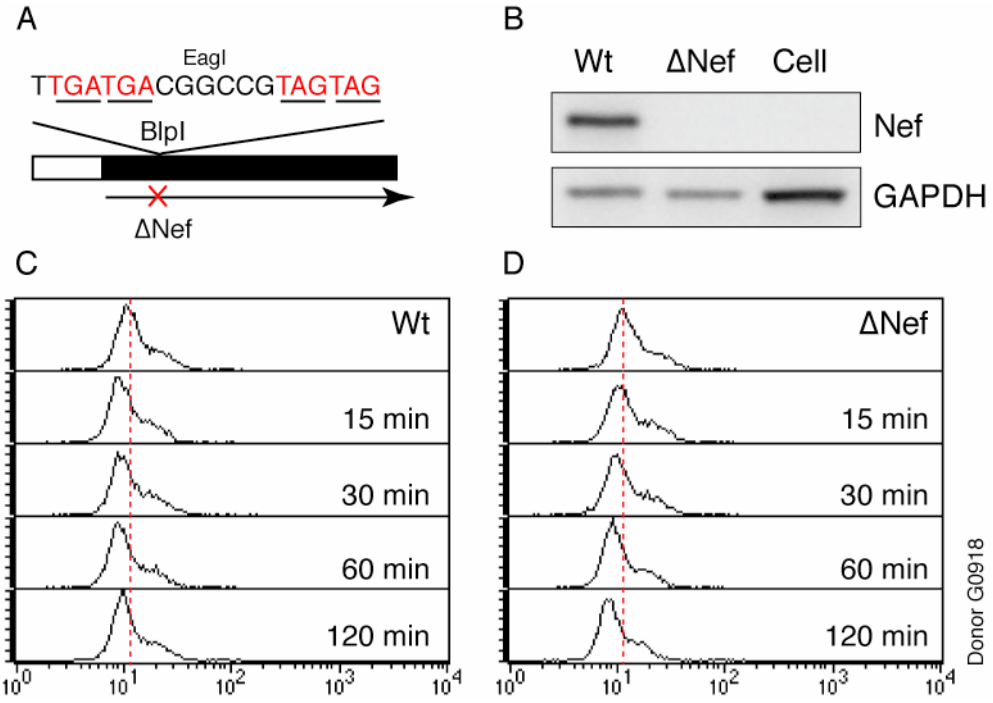

Figure S18. Depletion of Nef does not diminish the capacity of HIV-1 particles to mediate actin changes

HIV-1 Nef has been proposed to possibly depolymerize the cortical actin because of the observation that actin inhibitors diminish the positive effects of Nef on viral infectivity (Campbell et al., 2004). To determine whether Nef participates in viral Env-mediated actin activity, we depleted Nef from the virion particle and tested possible Nef effects on actin depolymerization. (A) The HIV-1 Nef gene was deleted from the HIV-1_{NL4-3} genome by insertion of a short oligonuclotide (with four stop codons) into the Nef ORF. (B) Nef negative viruses (ΔNef) were generated and cell lysates from transfection were used for western blot to confirm Nef deletion. The blot was probed with rabbit polyclonal anti-Nef antiserum (Shugars et al., 1993). GAPDH was used as a loading control and probed with goat polyclonal antibodies to GAPDH. (C, D) 100 ng of the wild type virus (Wt) and ΔNef virus was used to treat resting CD4 T cells to detect effects on actin changes, monitored by FITC-Phalloidin staining.

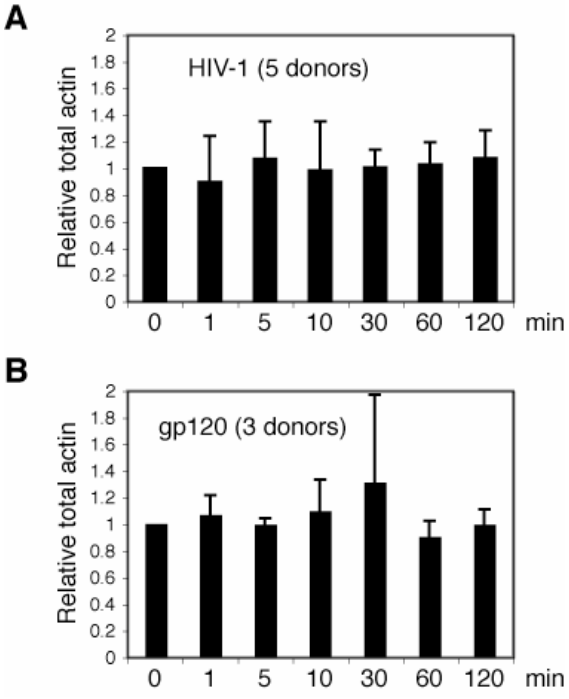

Figure S19. Total actin levels in HIV-1-infected and gp120-treated resting CD4 T cells

To determine whether the F-actin depolymerization trigged by binding of gp120 resulted from a loss of total actin protein, resting CD4 T cells purified from eight donors were either infected with HIV-1 (A) or treated with gp120 (B). The amount of total actin present in cells was measured by SDS-PAGE and Western blot using an anti-human actin antibody. Using densitometric quantification, the relative actin levels were determined by assigning the control (“0”, uninfected and untreated) a value of "1".

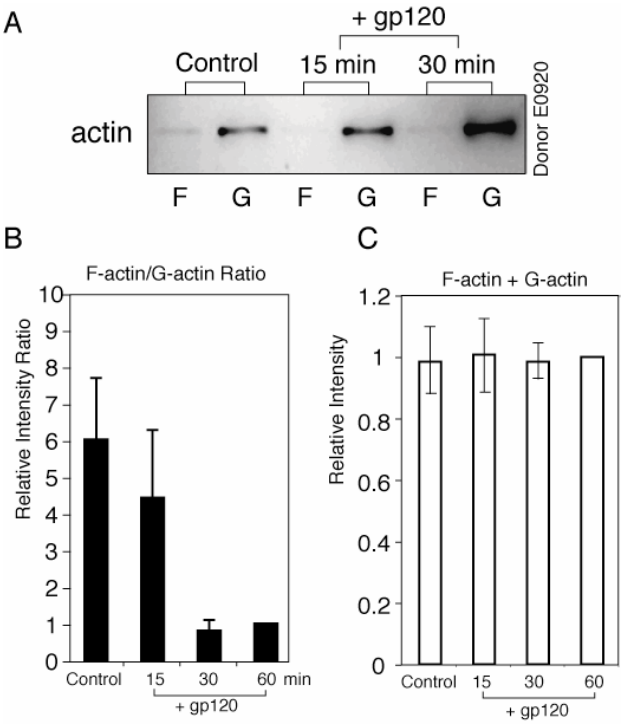

Figure S20. Cytoskeletal actin fractionation of resting CD4 T cells treated with gp120

Cells were treated with gp120 and then homogenized with F-actin stabilization buffer. F-actin (F) was separated from G-actin (G) by ultracentrifugation. F-actin in the pellet and G-actin in the supernatant were measured by SDS-PAGE and Western blot using an anti-human actin antibody. (A) is a representative image of cytoskeletal actin fractionation of resting CD4 T cells treated with gp120. (B) is the summary of the F/G-actin fractionation assay using gp120-treated resting CD4 T cells. Four independent cytoskeletal actin fractionation assays were performed. Densitometric quantification of the amount of F-actin in the pellet and G-actin in the supernatant was achieved by Western blot using an anti-human actin antibody. The relative ratio of F-actin to G-actin was determined by assigning the 60 minute-treated sample a value of "1". For statistic analysis, a two-tailed Student's t-test was performed on the means of the control sample and the 30 minute-treated sample. The test resulted in a p-value of 0.006 at a pre-determined significance level of 0.05, suggesting that the difference is statistically significant. (C) is the combination of F-actin and G-actin in each sample from (B). The relative F-actin plus G-actin was determined by assigning the 60 minute-treated sample a value of "1". For statistic analysis, a two-tailed Student's t-test was performed on the means of the control sample and the 30 minute-treated sample. The test resulted in a p-value of 0.994 at a pre-determined significance level of 0.05, suggesting that the difference is not statistically significant.

Note: We observed that both HIV-1 infection and gp120 treatment of resting CD4 T cells can cause decreased staining with FITC-labeled phalloidin. Since phalloidin has a much higher affinity for F-actin than G-actin, decreased staining normally indicates depolymerization of F-actin. Nevertheless, it does not always reflect a net loss of F-actin, particularly in rare cases where there are F-actin binding competitors in cells that block phalloidin binding. To confirm that gp120 triggers actin depolymerization, we performed cellular fractionation to measure changes in the ratio of F-actin to G-actin following gp120 treatment. Cells were treated, and then lysed and centrifuged to separate F-actin (in the pellet) and G-actin (in the supernatant). Relative ratios of F-actin/G-actin were measured to monitor actin changes. As shown in Figure S19, we detected a decrease in the ratio of F-actin/G-actin with gp120 treatment, confirming that staining with FITC-phalloidin reflects F-actin depolymerization in resting CD4 T cells.

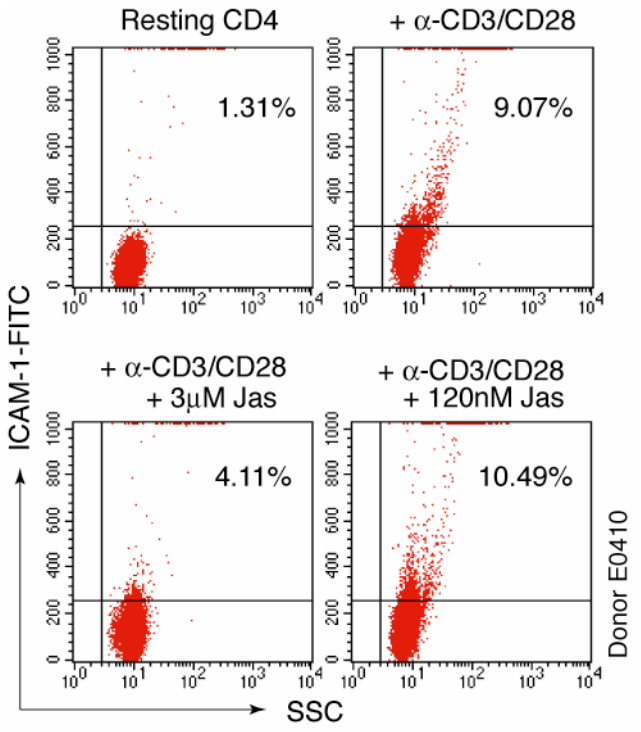

Figure S21. Effects of Jas on LFA-1 activation

Resting CD4 T cells were left untreated (upper right and left) or treated with 3 μM (lower left) or 120 nM (lower right) Jas for 2 hours, washed, and then unstimulated (upper left) or stimulated with anti-CD3/CD28 beads and stained with human ICAM-1/Fc chimera, followed by incubation with a FITC-labeled mouse anti-human Fc antibody. Stained cells were analyzed by flow cytometry.

Note: We decided to use the F-actin stabilizing agent Jasplakinolide (Jas) (Bubb et al., 2000) to inhibit HIV envelope-mediated actin depolymerization and to determine whether this would affect HIV latent infection. However, given that the actin cytoskeleton is also involved in T cell activation, Jas may affect HIV replication indirectly by affecting T cell activity. For instance, the actin cytoskeleton is known to be the driving force for receptor clustering and the formation of the supramolecular activation cluster (SMAC) during T cell activation (Wulfing and Davis, 1998). This process involves the actin-dependent activation of LFA-1 (Dustin and Springer, 1989), which is required for sustained signaling to reach full T cell activation (Wulfing and Davis, 1998). Thus, we first examined the effect of Jas on T cell activity using activation of LFA-1 as a marker. T cells were pretreated with different concentrations (3 μM to 30 nM) of Jas for 2 hours, and then activated with anti-CD3/CD28 beads. Following T cell activation, activation of LFA-1 was measured by staining with ICAM-1, the ligand for active LFA-1. Our data confirmed that T cell activation induces LFA-1 activation (upper right), and treatment of T cells with 3 μM Jas greatly inhibited LFA-1 activation (lower left). However, treatment of T cells with Jas at 120 nM or lower dosages had no detectable inhibition on LFA-1 activation (lower right).

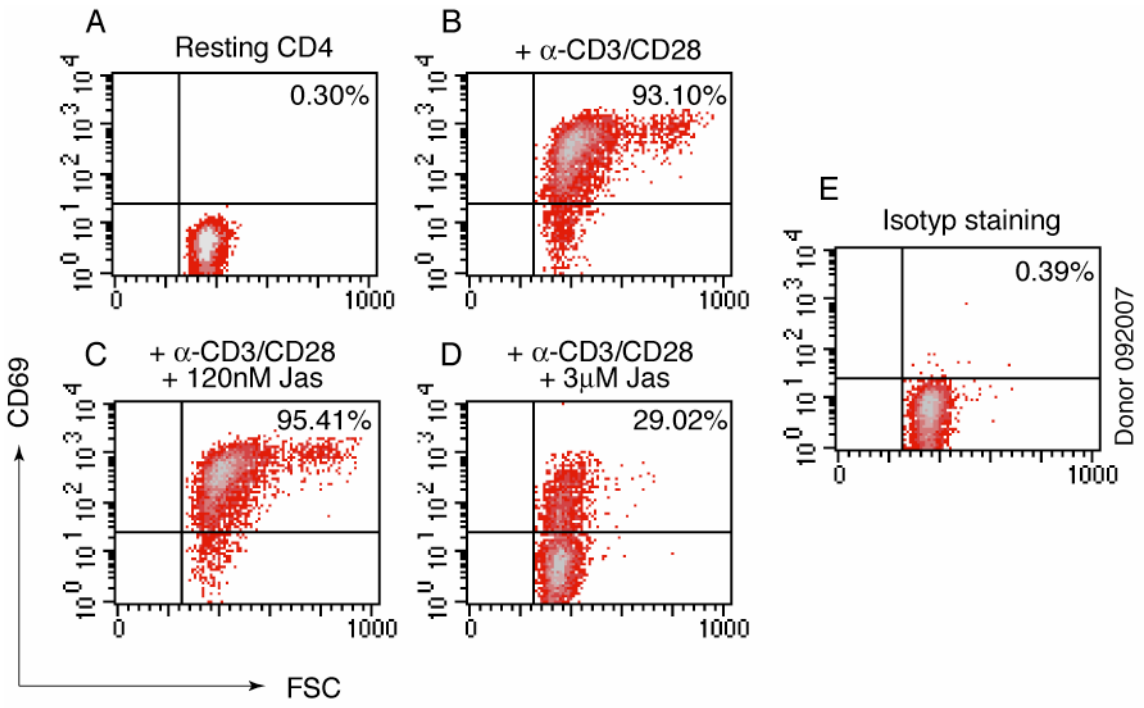

Figure S22. Effects of Jas on CD69 expression following T cell activation

We decided to use the F-actin stabilizing agent Jasplakinolide (Jas) to inhibit HIV envelope-mediated actin depolymerization and to determine whether this would affect HIV infection. However, given that the actin cytoskeleton is also involved in T cell activation, Jas may affect HIV replication indirectly by affecting T cell activity. Thus, we also examined the effect of Jas on T cell activity using expression of CD69 as an additional marker. T cells were pretreated with different concentrations (3 μM to 30 nM) of Jas for 2 hours, and then activated with BD anti-CD3/CD28 IMag particles. Following T cell activation, at 20 hours, activation of CD69 was measured by staining with PE-labeled anti-human CD69 monoclonal antibody. Our data confirmed that T cell activation induces CD69 expression (B), and treatment of T cells with 3 μM Jas greatly inhibited CD69 expression (D). However, treatment of T cells with Jas at 120 nM or lower dosages had no detectable inhibition on CD69 activation (C). Isotype control staining is shown in (E).

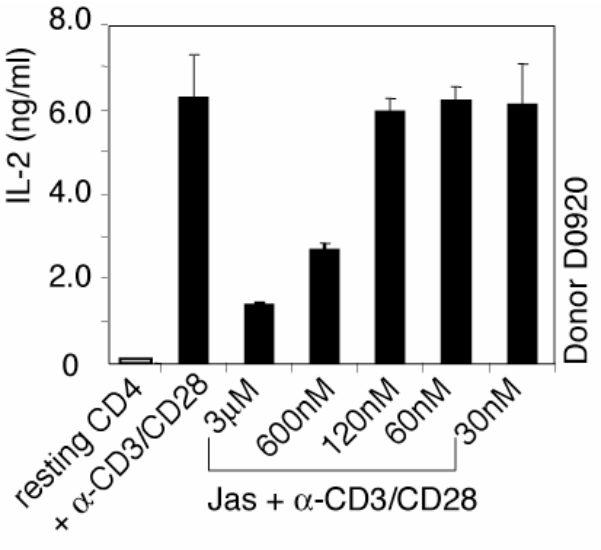

Figure S23. Effects of Jas on IL-2 secretion

Resting CD4 T cells were treated for 2 hours with various concentrations of Jas as indicated, and then washed and activated with anti-CD3/CD28 beads (4 beads per cell). Secretion of IL-2 in the supernatant was measured by IL-2 ELISA. Shown is IL-2 secretion at day 2 following activation. Jas-untreated, unactivated (the first lane from the left) or Jas-untreated, activated cells (the second lane from the left) were used as controls.

Note: We used the F-actin stabilizing agent Jasplakinolide (Jas) to inhibit HIV envelope-mediated actin depolymerization and to detect whether this would affect HIV latent infection. To determine the Jas dosage that minimally affects T cell activation, we used secretion of IL-2 as an indicator for effects of Jas on T cell activity. We confirmed that at 120 nM and below, Jas had no detectable inhibition on IL-2 secretion although at 600 nM and above it inhibited IL-2 expression (Figure S23). Effects of Jas on T cell activity were further tested by cell cycle analysis. At 3 μM, Jas arrested cells in the S phase, whereas at 120 nM, no cell cycle arrest was observed (data not shown). From these results, we determined that a Jas concentration of 120 nM or below could be used to test its effects on HIV replication.

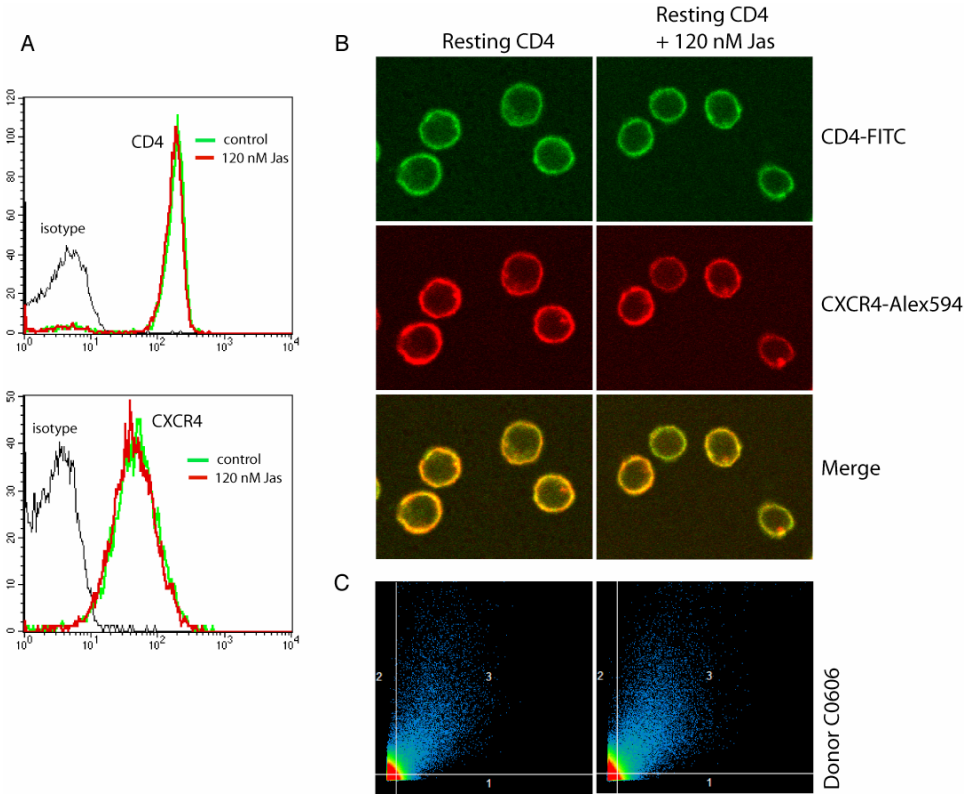

Figure S24. Effects of 120 nM Jas on CD4 and CXCR4 distribution on resting CD4 T cells

(A) Resting T cells were left untreated (green line) or treated with 120 nM Jas for 2 hours (red line), and then stained with FITC-labeled anti-human CD4 (top panel) or PE-labeled anti-human CXCR4 antibodies (bottom panel), and then analyzed by flow cytometry. Isotype staining is shown as the grey line. (B) Jas-treated (right panel) or untreated (left panel) cells were also fixed and stained with a FITC-labeled anti-human CD4 monoclonal antibody and a biotin-labeled anti-human CXCR4 monoclonal antibody followed by incubation with streptavidin-labeled Alexa Fluor-594. Cells were analyzed by confocal microscopy. (C) is a CD4/CXCR4 co-localization analyses of the samples in (B). 40 untreated and 54 Jas-treated cells were randomly selected for this analysis.

Note: The inhibition of HIV-1 latent infection by Jas could be due to its inhibition on CD4/CXCR4 receptor clustering or fusion which has been suggested to be actin dependent (Iyengar et al., 1998; Pontow et al., 2004). However, using 120 nM of Jas, we did not detect significant differences on CD4/CXCR4 distribution and co-localization. Our data also appear to support that in T cells, in the absence of HIV infection, a significant fraction of CD4/CXCR4 may have already formed a complex cycling between intracellular compartments and the cell surface (Zaitseva et al., 2005).

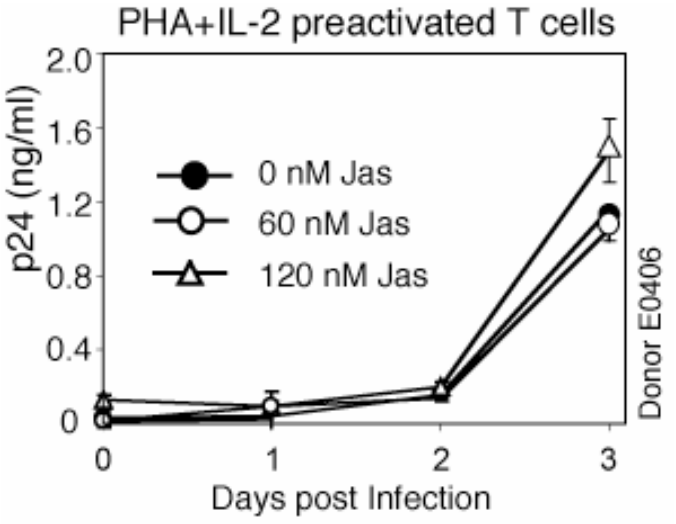

Figure S25. Lack of Jas inhibition of HIV replication in pre-activated T cells

Resting T cells were pre-activated with PHA plus IL-2 for 1 day, and then treated with different concentrations of Jas for 2 hours, washed, infected with HIV for 2 hours, washed, incubated for 3 days. Viral replication was measured by p24 release into the supernatant.

Note: At 120 nM, Jas inhibited HIV-1 infection of resting CD4 T cells (Figure 4A). However, at the same dosage, Jas did not inhibit HIV-1 infection of pre-activated CD4 T cells. It is possible that binding of Jas to F-actin competitively inhibits viral association with F-actin, and thus inhibits uncoating or reverse transcription. However, in activated T cells, the cell cycle regulates actin dynamics, and because 120 nM Jas does not inhibit the cell cycle, new actin filaments in cycling cells are likely free of Jas binding and inhibition.

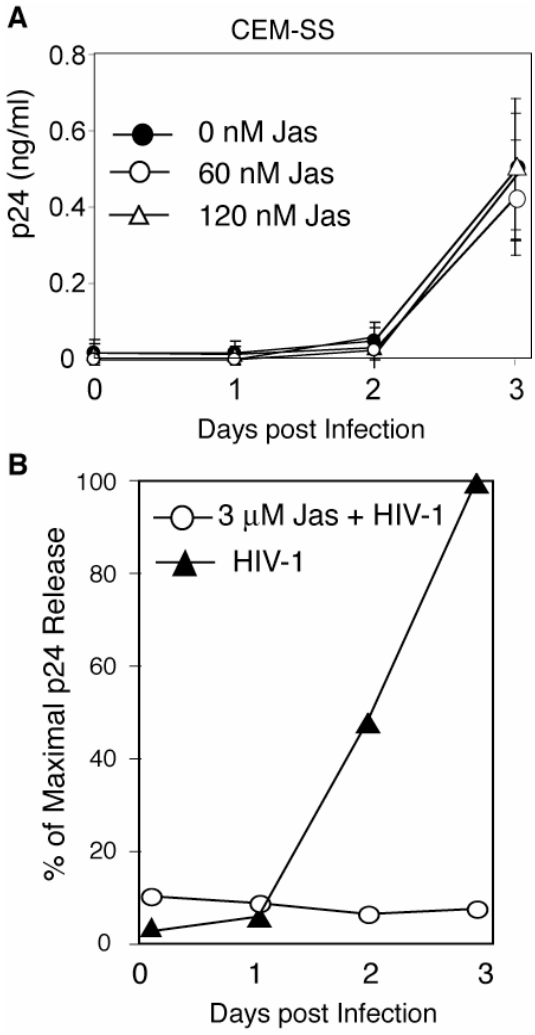

Figure S26. Effects of Jas on HIV-1 infection of transformed cells

CEM-SS cells were treated with Jas for 2 hours, washed, infected with HIV-1 for 2 hours, washed, and then cultured in fresh medium. Viral replication was monitored by measuring viral p24 release in the supernatant for 3 days. At 120 nM and below, Jas has no inhibition of viral replication (A). At 3 μM of Jas, viral replication was inhibited (B). At this dosage, the cell cycle was also inhibited, judged by DNA/RNA staining and flow cytometry analysis (data not shown).

Note: We demonstrate that 120 nM Jas diminishes HIV-1 infection of resting CD4 T cells (Figure 4A). It is possible that in the absence of cell cycle or cellular stimulation, cytoskeletal actin, particularly the cortical actin, in resting T cells could represent a restriction for the virus. However, for transformed cells, we did not observe inhibition of HIV-1 replication by 120 nM Jas (Figure S26A). It is likely that at 120 nM, Jas does not inhibit the cell cycle or cell cycle-mediated actin remodeling. At a higher dosage (3 μM), however, when the cell cycle was arrested, Jas did inhibit HIV replication in CEM-SS (Figure S26B).

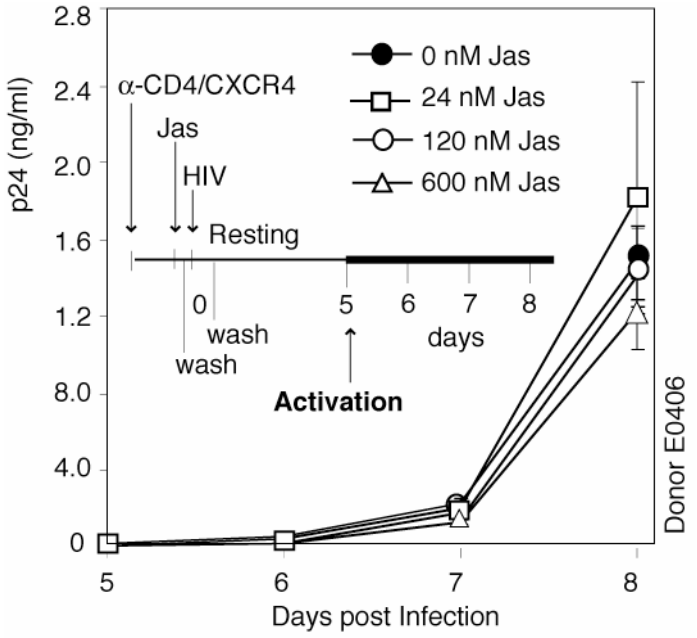

Figure S27. Lack of Jas inhibition of viral replication in resting CD4 T cells stimulated with anti-CD4/CXCR4 magnetic beads

Cells were pre-stimulated with anti-CD4/CXCR4 beads (2 beads per cell), then treated with various concentrations of Jas for 2 hours, washed, infected with HIV for 2 hours, washed, incubated for 5 days, and then activated by anti-CD3/CD28 magnetic beads (2 beads per cell). Viral replication was measured by p24 release into the supernatant.

Note: While both the 600 nM and 120 nM Jas inhibited HIV-1 latent infection of resting CD4 T cells (Figure 4A), at the same dosages, Jas did not inhibit HIV-1 infection of resting CD4 T cells pre-stimulated with anti-CD4/CXCR4 beads. It is likely that CD4/CXCR4 stimulation triggers dynamic actin change. The reorganization of F-actin will likely generate new filaments that are free of Jas binding and inhibition.

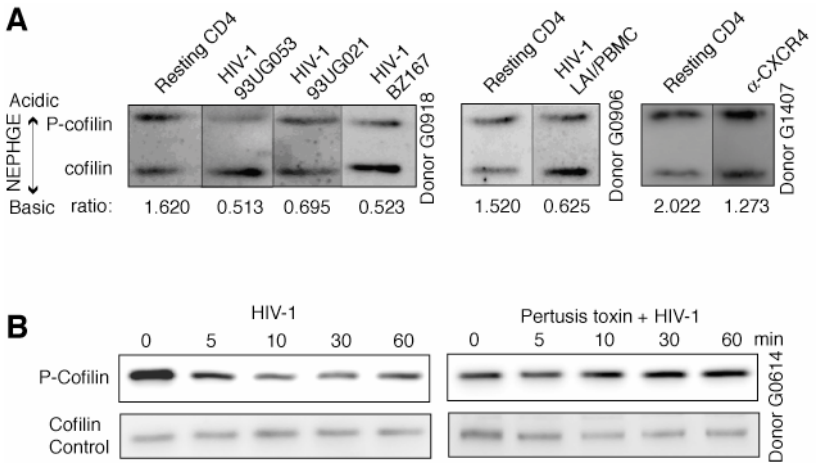

Figure S28. Activation of cofilin by multiple primary HIV-1 isolates

(A) Resting CD4 T cells were treated with multiple primary isolates of HIV-1 or anti-CXCR4 beads for 1 hour, and then analyzed by NEPHEGE-Western blot as described in Figure 5I (O'Farrell et al., 1977). The relative ratio of P-cofilin and active cofilin was indicated at the bottom. (B) is a repeat of Figure 5G and 5H in another donor.

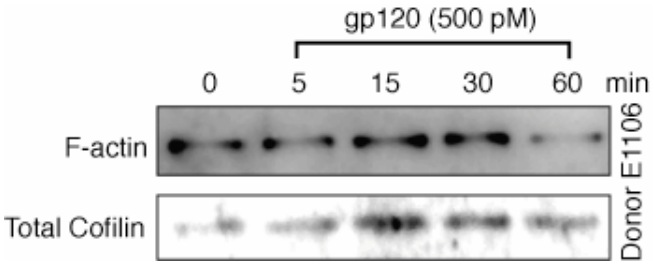

Figure S29. Activation of cofilin by gp120 promotes cofilin association with actin cytoskeleton

To demonstrate the association of active cofilin with F-actin in gp120-stimulated resting T cells, we fractionated F-actin before and after gp120 treatment. Cells were treated with gp120IIIB (500 pM), and then the F-actin fraction were prepared from fractionation of gp120-treated resting T cells, and analyzed by Western blot for actin (upper band) or cofilin (lower band). We observed low-level cosedimentation of cofilin with F-actin in un-treated resting T cells, and upon gp120 stimulation, there was an increase in cofilin association with F-actin, followed by a decrease in F-actin at 1 hour.

.

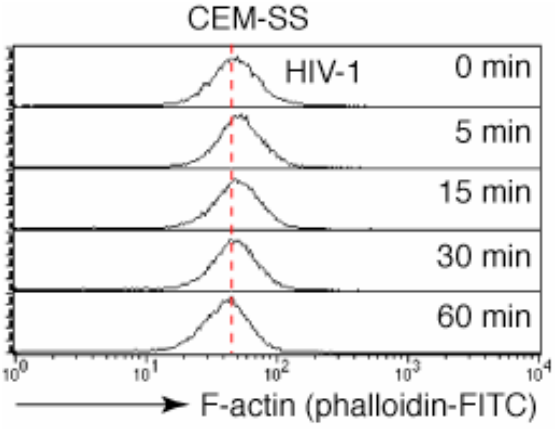

Figure S30. HIV-1 does not trigger actin depolymerization in transformed CEM-SS cell line

CEM-SS cells were treated with HIV-1 (100 ng p24 for 1 million cells) for various times. Cells were fixed, permeabilized and stained with FITC-phalloidin, and then analyzed by flow cytometry.

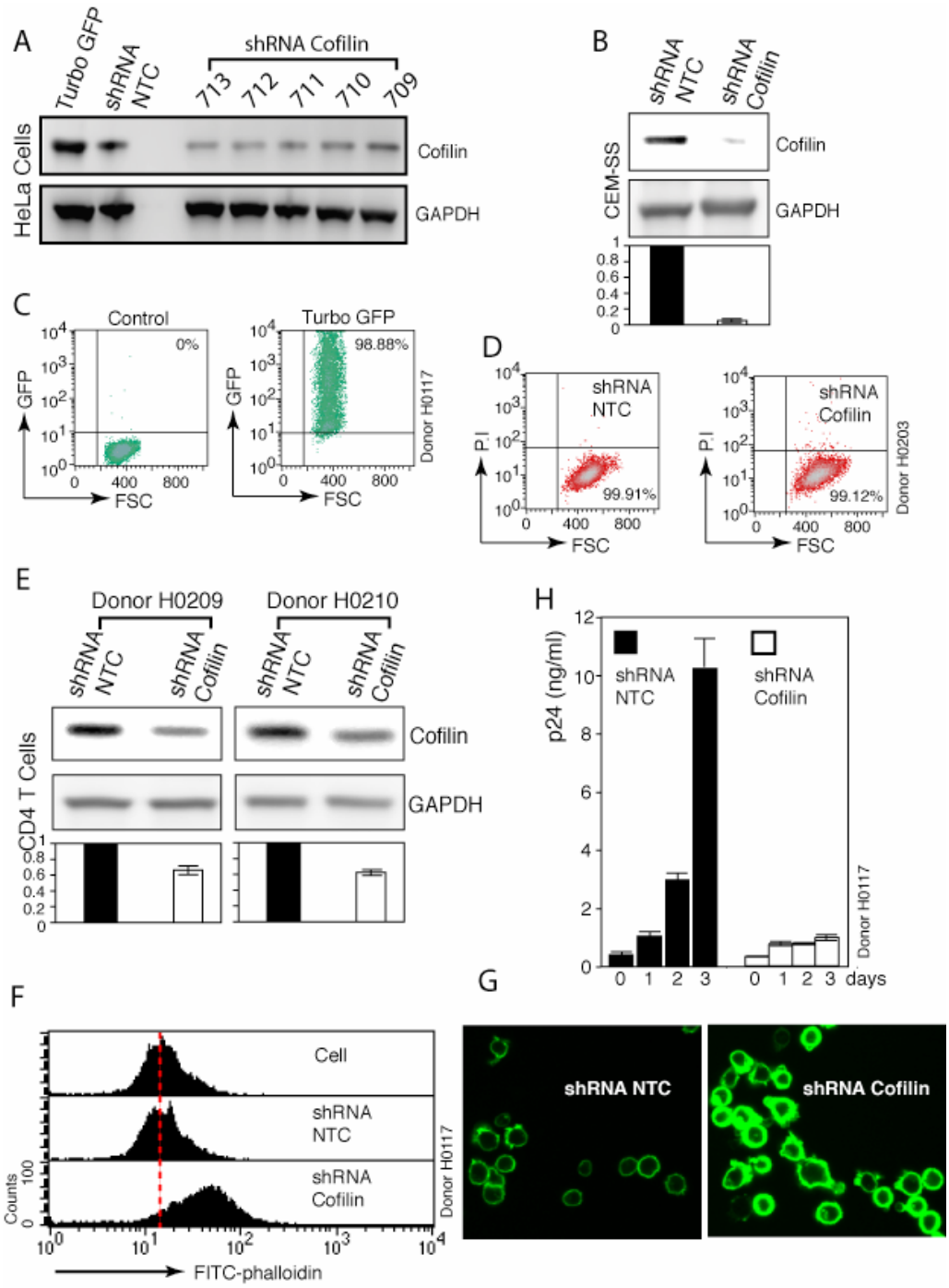

Figure S31. The study of shRNA knockdown of cofilin in primary human CD4 T cells.

To determine the requirement for cofilin activity in HIV-1-mediated actin change and viral infection, we tried to suppress cofilin expression in human CD4 T cells utilizing small interfering RNA (siRNA). The siRNA knockdown of cofilin has been

achieved in multiple cell lines (Hotulainen et al., 2005; Mouneimne et al., 2004; Sidani et al., 2007). We tested short hairpin RNAs (shRNA) that have been commonly used to silence genes by utilization of the RNA interference (RNAi) pathway. We acquired five cofilin-shRNA plasmids from Sigma (cofilin713, cofilin712, cofilin711, cofilin710, cofilin709), as well as a scrambled, non-targeting control shRNA vector (NTC) that activates the RNAi pathway but does not target any known human gene. Additionally, a Turbo GFP control vector containing the green fluorescent protein (GFP) was used as a control for measuring the transduction efficiency by the shRNA vectors. These plasmids also contain a puromycin resistance gene (from pLKO.1-puro) for the selection of stably transduced cells.

We first transiently transfected these vector DNAs into HeLa cells to test their effectiveness in knocking down cofilin. As shown in Figure S31A, at 24 hours post transfection, cells were harvested and analyzed by Western blot with antibodies against cofilin or GAPDH for loading control. We observed cofilin decrease by all five cofilin-shRNA plasmids. Based on these data, the plasmid cofilin712 was selected to produce viral particles to introduce the shRNA construct into human CD4 T cells (See Supplemental Methods).

Effective knockdown of cofilin by siRNA has been achieved in multiple cell lines (Hotulainen et al., 2005; Mouneimne et al., 2004; Sidani et al., 2007), although severe depletion or complete knockout of this gene appears to be lethal (Aizawa et al., 1995). As shown in Figure S31B, the cofilin shRNA is capable of knocking down over 90% of cofilin in a human T cell line, CEM-SS. In this experiment, we transduced CEM-SS with the vector carrying cofilin712 or the control NTC shRNA. Following transduction for 24 hours, cells were lysed and analyzed by Western blot as described in S31A. Nevertheless, the severe knockdown of 90% cofilin in CEM-SS triggered massive cell death (data not shown).

We then attempted to use the shRNA vector to knock down cofilin in human resting CD4 T cells. For viral delivery of shRNA, we first cultured resting CD4 T cells in cytokines such as IL-4 (10 ng/ml) for 4 days (Unutmaz et al., 1999), and then transduced them with the vector carrying cofilin shRNA. After one to two weeks, cells were harvested and analyzed by Western blot. We did not observe significant decrease in cofilin (data not shown). Similar difficulty in knockdown of certain mouse genes in primary naïve T cells has also been reported (McManus et al., 2002). These authors tested an alternative approach by transient stimulation of the T cell receptor with a cognate ovalbumin (OVA) peptide, and showed that it was effective in siRNA knockdown of genes in primary mouse T cells. Additionally, it was also shown that transient stimulation of the T cell receptor by antibodies followed by subsequent resting can permit retroviral transduction of primary human T cells (Schrager and Marsh, 1999).

We took advantage of these previous findings to establish a method for cofilin knockdown in primary human CD4 T cells. Resting CD4 T cells were transiently stimulated with anti-CD3/CD28 beads (1 -2 beads per cell) for 12 hours, then transduced with the shRNA vector for cofilin or NTC. Following transduction, the beads were removed at 12 hours, and cells were returned to resting for 2 days

and selected in puromycin (1 μg/ml). As shown in Figure S31C, using the Turbo GFP vector as a control, we can achieve 98% transduction efficiency. In this experiment, cells were transduced with Turbo GFP vector for 12 hours. Cells were then rested and selected in puromycin for 2 days. Following purification by centrifugation in lymphocyte separation medium, viable cells were run on flow cytometer to detect GFP-positive cells. The control was cells identically transduced with NTC.

We also transduced T cells with the cofilin shRNA vector using the same approach. Following transduction and resting, 99% of the cells recovered are viable, based on propidium iodide staining and flow cytometry analysis (Figures S31D). A fraction of these cells were also taken for Western blot analysis to confirm cofilin knockdown. As shown in Figure S31E, we were able to reduce cofilin to 66% and 63% respectively in the two donors tested. Further phonotypic characterization of the cofilin knockdown cells demonstrated that these cells had a higher level of F-actin, based on FITC-phalloidin staining and flow cytometry analysis (geometric mean of florescence, 37.16 versus 15.13, 10,000 cells) (Figure S31F). Confocal microscopy showed that the accumulation of F-actin mainly occurred in the cortical region (Figures S31G). Direct measurement of the cortical actin intensity in 100 randomly selected cells confirmed that the difference is statistically significant (data not shown). These data are in agreement with a previous finding that knockdown of cofilin reduces actin depolymerization rate, which leads to an increase in F-actin and a decrease in actin dynamics (Hotulainen et al., 2005).

We also infected the cofilin knockdown cells with HIV-1. As shown in Figure S31H, following transduction and resting, cells were infected with HIV-1 for 2 hours (0.02 $TCID50/_{Rev\text{-}CEM}$ per cell). Viral replication was monitored for three days by the p24 release into the medium following T cell activation at 24 hours. We observed inhibition of HIV-1 replication in the cofilin knockdown cells.

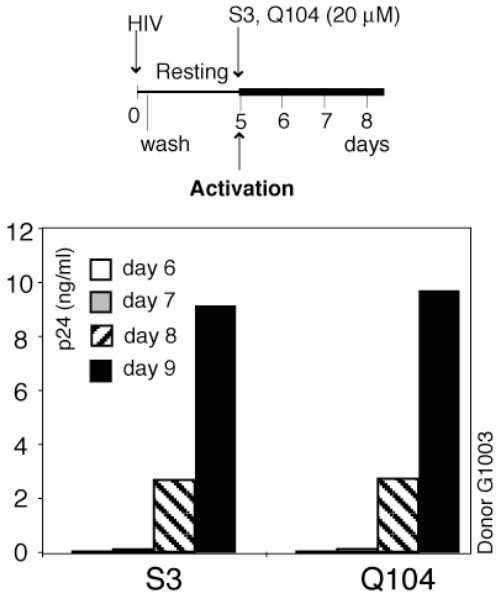

Figure S32. S3 peptide does not enhance viral replication when used during T cell activation

Resting CD4 T cells were incubated with S3 peptide (20 μM) after HIV-1 infection and at day 5 during T cell activation with anti-CD3/CD28 beads (4 beads per cell). As a control, infected cells were identically treated with Q104 and activated. Shown is viral replication from day 6 to 9. Viral replication was enhanced when S3 was added prior to infection (Figures 6C to 6E), whereas viral replication was not significantly affected when S3 was added at the time of T cell activation (Figure S32), suggesting that the enhancement by S3 is unlikely the result of T cell activation by S3 or of the synergy between S3 and CD3/CD28 stimulation.

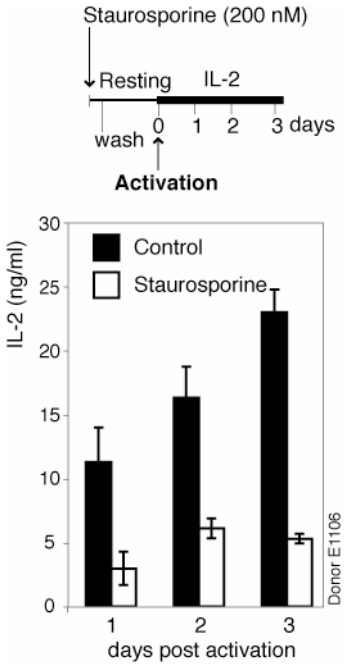

Figure S33. Inhibition of IL-2 secretion by staurosporine

Resting CD4 T cells were treated with staurosporine (200 nM) or DMSO (control) for 2 hours, and then washed and incubated for 1 day in the absence of the inhibitor. Cells were activated by anti-CD3/CD28 beads (4 beads per cell), and IL-2 in the supernatant was collected and measured by IL-2 ELISA.

Note: Staurosporine is a serine/threonine kinase inhibitor with preferential inhibition of phospholipid/Ca++ dependent protein kinases such as PKC (Tamaoki et al., 1986). Staurosporine is known to be one of the most potent inhibitors of T cell activation (Kubbies et al., 1989). To confirm that the observed enhancement of HIV-1 infection by staurosporine (Figure 7A) was not due to its enhancement of T cell activation, we performed an experiment similar to that of Figure 7A, with resting CD4 T cells treated identically with 200 nM staurosporine, incubated, and then activated. Using IL-2 in the culture supernatant as an indicator, our data indicated that brief treatment of resting CD4 T cells with 200 nM staurosporine inhibited IL-2 secretion (Figure S33), demonstrating that the enhancement of HIV-1 replication by staurosporine did not result from an enhancement of T cell activity.

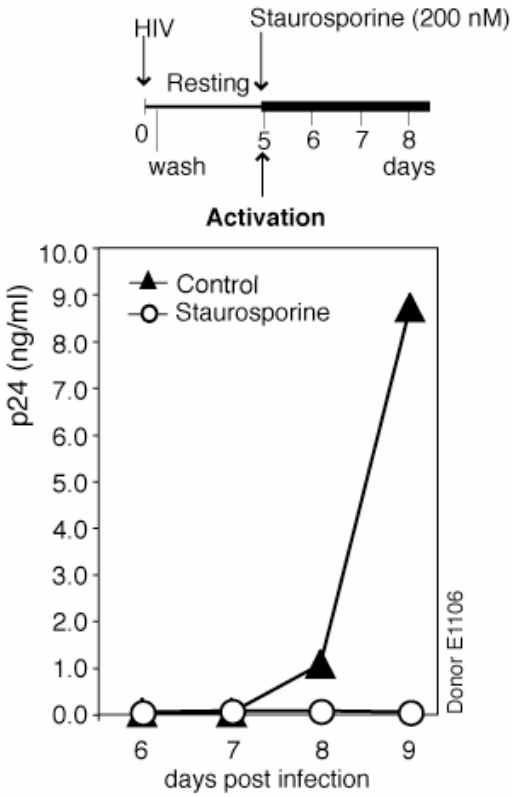

Figure S34. Inhibition of T cell activation and viral replication by staurosporine

Resting CD4 T cells were infected with HIV-1, washed, and then cultured for 5 days. At day 5, cells were activated by anti-CD3/CD28 beads (4 beads per cell) in the presence of 200 nM staurosporine. Viral p24 release was measured. Control cells were identically infected with HIV and activated in the absence of staurosporine.

Note: We observed that treatment of resting CD4 T cells with 200 nM staurosporine prior to infection greatly enhanced HIV-1 infection of resting CD4 T cells (Figure 7A). To further confirm that the observed enhancement was not due to its enhancement on T cell activation, we performed an experiment identical to that of Figure 7A with the modification that 200 nM staurosporine was added during T cell activation at day 5 rather than at 2 hours before infection. We observed complete inhibition of HIV-1 replication (Figure S34), likely as the result of inhibition on T cell activation by staurosporine.

Supplemental Experimental Procedures

Isolation of Resting CD4 T Cells From Peripheral Blood

All protocols involving human subjects were reviewed and approved by the George Mason University IRB and Chesapeake Research Review IRB. Peripheral blood mononuclear cells (PBMC) were obtained from healthy donors at the Student Health Center, George Mason University, Fairfax, VA and the NIH blood bank. Resting CD4 T cells were purified by two rounds of negative selection as previously described (Wu and Marsh, 2001). Purified cells were cultured in RPMI 1640 medium supplemented with 10% heat-inactivated fetal bovine serum (Invitrogen), penicillin (50 U/ml), and streptomycin (50 μg/ml). Cells were rested overnight before infection or treatment.

Virus Preparation and Infection of Resting CD4 T Cells

Virus stocks of HIV-1_{NL4-3} (Adachi et al., 1986) were prepared by transfection of HeLa cells with cloned proviral DNA as described (Wu and Marsh, 2001). We found that although HeLa cell generates lower titer, it has lower gp120 shedding than HEK293T cell (data not shown). Supernatant was harvested at 48 hours and filtered through an 0.45 μm nitrocellulose membrane. Virus titer ($TCID_{50}$) was measured by infection of a Rev-dependent indicator cell line, Rev-CEM, which was constructed through stable integration of a Rev-dependent GFP expression lentiviral vector into CEM-SS (Wu et al., 2007a). This Rev-CEM cell line has no background GFP expression, and gives titers close to those obtained using PBMC. HIV-1(KFS) was kindly provided by Dr. Eric Freed (Freed et al., 1992).

For infection of resting CD4 T cells, viruses were first titrated to determine the minimal level detectable by p24 ELISA. Unless specified, for most replication assays, $10^{3.5}$ to $10^{4.5}$ $TCID_{50}$ units of HIV-1 were used to infect 10^6 cells. The use of low viral dosages is important for the observation of the enhancement by the numerous stimulations described in the paper and for reducing possible activation of multiple G proteins. It has been demonstrated that at high chemokine concentrations, chemokine receptors can be promiscuously coupled to both PTX-sensitive G alpha *i* and insensitive G alpha *q* (Arai and Charo, 1996; Simon et al., 1991).

For the infection procedure, CD4 T cells were incubated with the virus for 2 hours, and then washed twice with medium to remove unbound virus. Infected cells were resuspended into fresh RPMI-1640 medium supplemented with 10% heat-inactivated fetal bovine serum, penicillin (50 U/ml), and streptomycin (50 μg/ml) at a density of 10^6 per ml and incubated for 5 days without stimulation. Cells were activated at day 5 with anti-CD3/CD28 magnetic beads at 4 beads per cell. For the viral replication assay, 10% of infected cells were taken at days 1, 3, 5, 6, 7, 8, and 9 post infection. Cells were pelleted and the supernatant was saved for p24 ELISA. Levels of p24 in the supernatant were measured using a Coulter HIV-1 p24 Assay Kit (Beckman Coulter) or a Perkin Elmer Alliance p24 antigen ELISA Kit (Perkin Elmer). Plates were kinetically read using an ELx808 automatic microplate reader (Bio-Tek Instruments) at 630 nm.

Pre-treatment of Resting CD4 T Cells With Inhibitors and Cytokines

Resting CD4 T cells were treated for 2 hours with pertussis toxin (Sigma) (100 ng/ml), damnacanthal (Biomol) (Faltynek et al., 1995) (1 μM), or piceatannol (Biomol) (Peters et al., 1996) (10 μM) and then infected with HIV-1. Following infection, cells were washed 2 to 3 times to remove cell-free virus and the inhibitors, cultured for 5 days in the absence of the inhibitors, and then activated with anti-CD3/CD28 magnetic beads (4 beads per cells).

For treatment of resting CD4 T cells with gp120 IIIB (Immuno Diagnostics), 10^6 cells were treated with gp120 IIIB for 12 hours and then infected with HIV-1. Following infection, cells were washed and continuously cultured for 5 days in the presence of gp120 and then activated with anti-CD3/CD28 beads (4 beads per cell).

Cells were treated with jasplakinolide (Invitrogen) (Bubb et al., 2000) for 1 to 2 hours or latrunculin A (Biomol) (Coue et al., 1987; Morton et al., 2000; Spector et al., 1983) for 5 minutes at various concentrations, washed twice with medium, and then infected with HIV-1.

For inhibiting CXCR4 signaling, a highly specific CXCR4 antagonist, AMD3100 , was used. This inhibitor specifically interacts with the three acidic residues (Asp171, Asp262, Glu288) in the main ligand binding pocket of CXCR4 (Gerlach et al., 2001; Schols et al., 1997). Resting CD4 T cells were briefly treated with AMD3100 (100 nM), and then treated with gp120.

Cells were treated with 200 nM of staurosporine (Biomol) (Tamaoki et al., 1986) for 2 hours, and then infected with HIV-1. Following infection, cells were washed twice to remove cell-free virus and the inhibitor. To detect effects of staurosporine on cofilin activation and actin depolymerization, cells were treated with 200 nM of staurosporine for various times, and then pelleted and lysed in NuPAGE LDS Sample Buffer (Invitrogen) for Western blot, or directly fixed and permeabilized for F-actin staining.

For activation of resting CD4 T cells with PHA (3 μg/ml) (Sigma) plus IL-2 (100 U/ml) (Roche Applied Science), cells were cultured in the presence of these agents for 1 day.

For cytokine stimulation of resting CD4 T cells, cells were cultured in IL-2 (200 U/ml) (PeproTech) or IL-7 (10 ng/ml) (PeproTech) for four days. It has been shown that certain lymphatic homeostatic cytokines such as IL-2 and IL-7 can promote low level HIV-1 replication through the inactivation of low molecular weight mass APOBEC3G (LMM A3G) (Ducrey-Rundquist et al., 2002; Kreisberg et al., 2006; Unutmaz et al., 1999). Cytokine-stimulated cells were either infected directly with HIV-1 or pre-stimulated for 12 hours with anti-CD3/CXCR4 beads (2 beads per cells) before infection. Cells were infected in the presence of the cytokines for 2 hours, washed, and then resuspended into fresh medium with the cytokines added. Cells were continuously cultured without further activation or activated at day 5 post infection with anti-CD3/CD28 beads (4 beads per cell). Low levels of viral replication were observed without T cell activation. Activation with anti-CD3/CD28 beads greatly enhanced viral replication.

Viral Fusion Assay

Viral fusion assays were performed as previously described (Cavrois et al., 2002). Briefly, viruses were generated by cotransfection of HeLa cells with three plasmids: pHIV-1_{NL4-3}, pAdvantage (Promega) and pCMV4-3BlaM-Vpr (kindly provided by Dr. Warner C. Greene) (in the ratio of 6:1:2). Supernatant was harvested at 48 hours post cotransfection, concentrated and then used for infection of resting CD4 T cells as suggested (Cavrois et al., 2002). For infection of resting CD4 T cells, 1750 ng (p24) of HIV-1(BlaM-Vpr) was used for 1 million cells. Flow Cytometry was performed using a Becton Dickinson LSR II (Becton Dickinson). β-lactamase and CCF2 measurements were performed using a 407nm violet laser with emission filters of 525/50 nm (green fluorescence) and 440/40 nm (blue fluorescence), respectively. Green and blue emission spectra were separated using a 505LP dichroic mirror. A UV laser was turned off during the analysis. Data analysis was performed using BD FACSDiva software, Version 4.1.1.

Pre-treatment of Resting CD4 T Cells With Synthetic Peptide

Synthetic peptide S3 (MASGVAVSDGVIKVFN) was derived from the N-terminal 16 amino acids of human cofilin. The control peptide, S3D (MADGVAVNDGVIKVFN), was derived from S3 with serine 3 mutated to Aspartic Acid (D), and Q104 (WAPESAPLQSQM) was derived from human cofilin residues 104 to 115 with lysine 112 and 114 mutated to glutamine. All peptides were synthesized by Celtek Peptides and conjugated to a penetratin peptide (RQIKIWFQNRRMKWKK) for intracellular delivery. Resting CD4 T cells were treated with S3, S3D or Q104 for 1 to 2 hours, and then infected with HIV-1. Following infection, cells were washed 2 to 3 times to remove cell-free virus and the peptides.

Conjugation of Antibodies to Magnetic Beads and Stimulation of Resting CD4 T Cells

Monoclonal antibodies against Human CD3 (clone UCHT1), CD28 (clone CD28.2), CD4 (clone PRA-T4) and CXCR4 (clone 12G5) were from BD Pharmingen (BD Biosciences). The anti-CD4, CXCR4 antibodies were selected for their shared epitopes with gp120. The CD4 antibody, clone RPA-T4, binds to the D1 domain of the CD4 antigen and is capable of blocking gp120 binding to CD4 (Dalgleish et al., 1984), whereas the anti-CXCR4 antibody, clone 12G5, interacts with the CXCR4 extracellular loops 1 and 2, which partially overlap domains for HIV-1 coreceptor function (Lu et al., 1997). The 12G5 antibody has also been shown to block HIV-1-mediated cell fusion (Hesselgesser et al., 1998) and CD4-independent HIV-2 infection (Endres et al., 1996). For conjugation, 10 μg of antibodies were conjugated with 4 x 10^8 Dynal beads (Invitrogen) for 30 minutes at room temperature. Free antibodies were washed away with PBS-0.5% BSA, and the magnetic beads were resuspended in 1 ml of PBS-0.5%BSA. For stimulation of resting CD4 T cells, antibody conjugated beads were washed twice, and then added to cell culture and rocked for 5 minutes. For observing

enhancement of viral replication by anti-CD4/CXCR4 beads stimulation, cells were pre-stimulated with the beads (2 beads per cell) overnight, then infected with HIV-1. Conjugation of anti-CD4, CXCR4 antibodies with streptavidin-labeled BD IMag particles (BD Biosciences) was carried out using washed particles and biotin-labeled anti-CD4, CXCR4 antibodies (BD Biosciences). The mixture was incubated for 30 minutes at room temperature with gentle shaking, washed three times, and resuspended into PBS-0.1% BSA.

Cell cycle analysis by 7-AAD and PY staining

Resting CD4 T cells (10^6) were treated with gp120 IIIB (Immuno Diagnostics) (50 nM) or anti-CD4/CXCR4 BD IMag particles (BD Biosciences) for 5 days. Cells were suspended in 1 ml of 0.03% saponin in PBS and then incubated in 20 μM 7-amino-actinomycin D (Sigma) for 30 minutes at room temperature in the dark. Cells were kept on ice for at least 5 minutes, pyronin Y (Sigma) was added to a final concentration of 5 μM and the cells were then incubated for 10 minutes on ice. Stained cells were directly analyzed by flow cytometry on a FACSCalibur (Becton Dickinson).

Cytoplasmic and nuclear DNA fractionation

The cell fractionation protocol was modified from Lassen *et al* (Lassen et al., 2006). Briefly, cells were pelleted at 270 x g for 5 minutes in a microfuge at 4ºC, washed once with ice-cold PBS, resuspended into ice-cold cell lysis buffer (10 mM Tris.Cl, PH 7.5, 140 mM NaCl, 5 mM KCl, 1% EDTA, 1% NP-40) and incubated on ice for 5 to 10 minutes, and then centrifuged at 270 x g for 5 minutes at 4ºC to pellet the nuclei. Supernatant was removed and centrifuged at 13,000 x g for 5 minutes to remove nuclear contamination. Nuclear pellet was washed once with ice-cold cell lysis buffer and then dissolved in DNA extraction lysis buffer (SV Total RNA Isolation System, Promega). Both cytoplasmic and nuclear DNA was extracted using SV Total RNA Isolation System and dissolved in 100 μl of H20. Equal volumes of cytoplasmic and nuclear DNA were used for PCR amplification for viral late DNA, or for amplification of β-actin pseudogene as a control for nuclear DNA, using the actin primer from Quantu mRNA β-actin Internal Standards (Ambion). For cytoplasmic DNA control, known copies of an exogenous plasmid DNA, pNL-GFP-RRE-(SA) (Wu et al., 2007b), were added into the cell lysis buffer during cell lysis. Both cytoplasmic and nuclear DNA were amplified with primers for the GPF gene to determine possible contamination of the nuclear DNA by the cytoplasmic DNA.

FITC-Phalloidin Staining of F-actin and Flow Cytometry

One to two million cells were stimulated with HIV-1 or gp120 IIIB (Microbix Biosystems) in 2 ml round bottom tubes, incubated at 37ºC in an Eppendorf Thermomixer with gentle agitation (600 to 1200 rpm) to prevent cell settling at the bottom. F-actin staining using FITC-labeled phalloidin (Sigma) was carried out according to the manufacturer's recommendation with minor modifications. Briefly, each staining was carried out using 1-2 $x10^6$ cells. Cells were pelleted,

fixed and permeabilized with CytoPerm/Cytofix buffer (BD Bioscience) for 20 minutes at room temperature, washed with cold Perm/Wash buffer (BD Bioscience) twice, followed by staining with 5 μl of 0.3 mM FITC-labeled phalloidin for 30 minutes on ice in dark. After washing twice with cold Perm/Wash buffer, cells were resuspended in 1% paraformaldehyde and analyzed on a FACSCalibur (BD Biosciences).

Staining of LAF-1 Activation on Resting CD4 T Cells

Half a million CD4 T cells in 500 μl culture medium were treated with 5 μl of human IgG (Jackson Immuno Research) to block non-specific staining. Cells were stained with 10 μl (50 μg/ml) of human ICAM-1 Fc chimera (R&D System) for 20 minutes at 4ºC. Cells were washed and blocked by 5 μl of mouse IgG (Jackson ImmunoResearch), followed by the addition of 10 μl of FITC-labeled mouse anti-human Fc (Jackson Immuno Research), and incubated for 20 minutes at 4ºC. Finally, cells were washed and resuspended in 500 μl of 1% paraformaldehyde for flow cytometry.

Confocal Microscopy

Stained cells were imaged using a Zeiss Laser Scanning Microscope, LSM 510 META, with a 40 NA 1.3 or 60 NA 1.4 oil DIC Plan-Neofluar objective. Samples were excited with two laser lines, 488 nm for GFP and 543 nm for Alexa 594. Images were simultaneously recorded in three channels: channel one, fluorescent emissions from 505 to 530 nm for GFP (green); channel two, emissions from 580 to 650 nm for Alexa 594 (red); channel three, DIC. Images were processed and analyzed by the LSM 510 META software.

For quantification of confocal images, individual T cells in confocal images were automatically detected using a customized Matlab script (Mathworks, Inc.). Changes in staining intensity were selected by edge detection, and the binary edge detection mask was then dilated and smoothed to yield an outline for each cell. Fluorescent intensities were determined per cell by calculating the sum of the values for pixels within each outline.

Real Time PCR Amplification of Viral DNA

Quantitative real-time PCR analyses of viral DNA and 2-LTR circles were carried out by using Bio-Rad iQ5 real-time PCR detection system as described previously (Wu and Marsh, 2003), using the forward primer, 5'LTR-U5: 5'-AGATCCCTCAGACCCTTTTAGTCA-3'; the reverse primer, 3' gag: 5'-TTCGCTTTCAAGTCCCTGTTC-3'; the probe, FAM-U5/gag: 5'-(FAM)-TGTGGAAAATCTCTAGCAGTGGCGCC-(BHQ)-3'. The DNA standard used for both late DNA and 2-LTR circle quantification was constructed by using a plasmid containing a complete 2 LTR region (pLTR-2C, cloned by amplification of infected cells with 5'-TGGGTTTTCCAGTCACACCTCAG-3' and 5'-GATTAACTGCGAATCGTTCTAGC-3'). Measurement was run in triplicate ranging from 1 to 10^6 copies of pLTR-2C mixed with DNA from uninfected cells. For the measurement of HIV-1 DNA in the shRNA lentiviral vector transduced cells, the following primers were used: 5'-

GCGGGAGAATGATAATGGAGAAAGG-3'; 5'-
GGCCTGTGTAATGACTGAGGTGTT-3'; the probe: 5'-(FAM)-
TCAGCACAAGCATAAGAGATAAGGTGCAGA-(BHQ)-3'.

Alu-PCR Amplification of Viral Integration

To construct the Alu-PCR DNA standard, a lentiviral vector pNLneo was first constructed by inserting a 1.3 kb fragment of pMSCVneo (Clontech) (containing the PKG promoter and the neomycin resistance gene) into a lentiviral vector carrying the HIV-1_{NL4-3} LTRs at the two ends. The resulting plasmid, pNLneo, were used to generate lentivirus and used to infect HeLa cells, using a low multiplicity of infection 0.05 to 0.1. Following infection, cells were culture in 1 mg/ml of G418 for more than one month to ensure that unintegrated DNA is diminished and only integrated viral DNA remains. DNA from G418 resistant HeLa cells (HeLa-NLneo) were then extracted and copies of viral DNA was measured by real-time PCR as described above. The viral DNA copy number in HeLa-NLneo was determined to be approximately 1.4 copies per cell. DNA from HeLa-NLneo was diluted into uninfected HeLa cellular DNA to keep the number of Alu sites constant.

For measurement of integration, total genomic DNA was purified and PCR amplified using Alu-forward primer (5'-GCCTCCCAAAGTGCTGGGATTACAG -3') and Alu-gag-reverse primer (5'-GCTCTCGCACCCATCTCTCTCC-3') as previously described (O'Doherty et al., 2002). PCR reactions were set up using SuperTaq Plus Polymerase (Ambion) with a final reaction mix of 50 μl containing 2.5 mM of each of the dNTPS, 100 pm of Alu-forward primer, 100 pm gag-reverse primer and 2U of SuperTaq plus polymerase. The reaction was performed for 30 cycles at 94°C for 10S, 66.4°C for 20S and 68°C for 3 minutes. Background amplification from non-integrated viral DNA was also measured as controls, using the *Alu-gag-reverse* primer alone. Following the first round PCR amplification, an aliquot equivalent to one-fifth the volume of the Alu-PCR products was used for real-time PCR analysis of viral DNA as described above. Integrated viral DNA copy was calculated based on the Integrated viral DNA standard prepared from HeLa-NLneo

Cofilin and Phospho-cofilin Western Blot

One million CD4 T cells were lysed in NuPAGE LDS Sample Buffer (Invitrogen) followed by sonication. Samples were heated at 70ºC for 10 minutes before loading, and then separated by SDS-PAGE and transferred onto nitrocellulose membranes (Invitrogen). The membranes were washed in TBS for 5 minutes and then blocked for 30 minutes at room temperature with Starting Block blocking buffer (Pierce). The blots were incubated with either a rabbit anti-cofilin antibody (1:1000 dilution) (Cell Signaling) or a rabbit anti-phospho-cofilin (ser3) antibody (1:1000 dilution) (Cell Signaling) diluted in 5% BSA-TBST and rocked at room temperature for 1 hour or overnight at 4°C. The blots were washed three times for 15 minutes each and then incubated with goat anti-rabbit horseradish peroxidase-conjugated antibodies (KPL) diluted in 2.5% skim milk-TBST (1:5000)

for 1 hour. The blots were washed again three times for 15 minutes each and then developed with SuperSignal West Femto Maximum Sensitivity Substrate (Pierce). Images were captured with a CCD camera (FluorChem 9900 Imaging Systems) (Alpha Innotech) and analyzed and processed by NIH-Image Version 1.63.

F-actin/G-actin Fractionation and F-actin/cofilin Cosedimentation Assays

F-actin/G-actin cellular fractions were prepared using the F-actin/G-actin *in vivo* assay kit (Cytoskeleton). Briefly, 2 million resting CD4 T cells per sample were treated with 500 pM gp120 from 5 minutes to 1 hour. The cells were harvested by centrifugation at 2,000 g for 1 minute at 37ºC and then resuspended in 1.5 ml lysis buffer (50 mM PIPES pH6.9, 50 mM KCl, 5 mM $MgCl_2$, 5 mM EGTA, 5% (v/v) glycerol, 0.1% Nonidet P40, 0.1% Triton X-100, 0.1% Tween 20, 0.1% 2-mercapto-ethanol, 0.001% antifoam C, 4 μM tosyl arginine methyl ester, 15 μM leupeptin, 10 μM pepstatin A, 10 mM benzamidine and 1 μM ATP). The lysates were homogenized with a 200 μl fine orifice pipette and then held at 37ºC for 10 minutes. The lysates were then centrifuged at 420 x g for 5 minutes to remove cell debris and the supernatant was collected and centrifuged at 100,000 x g at 37ºC for 1 hour. Following centrifugation, the supernatant containing G-actin was saved and the pellet containing F-actin was resuspended in F-actin depolymerizing solution (10 μM cytochalasin D) and incubated on ice for 1 hour with occasional pipetting. Equal volumes of the supernatant and pellet fractions were used for SDS PAGE and Western blotting for actin. For the F-actin/cofilin cosedimentation assay, the F-actin pellet was directly resuspended in 1 x LDS sample buffer for SDS-PAGE and immunoblotting for cofilin and actin.

NEPHGE and Western Blot for Cofilin

One-dimensional nonequilibrium pH gel electrophoresis (NEPHGE) was performed as previously described (Nebl et al., 2004). Briefly, resting T cells were lysed in TKM buffer (50 mM Tris.Cl pH 7.6, 25 mM KCL, 5 mM $MgCL_2$, 1mM Na-Vandate, 5 mM NaF, 20 μg/ml leupeptin, 20 μg/ml aprotinin, 0.3 μM okadaic acid containing 0.5-1% NP-40) and sedimented at 20,800 x g for 10 minutes at 4ºC. Postnuclear fractions were collected and used for the detection of cofilin. NEPHGE was performed with 6%-focusing slab gel with 5% Ampholines pH 3 to 10 (Invitrogen). The gels were run for 1 hour at 100V, 2 hours at 250V and 2 hours at 300V, and then transferred onto nitrocellulose membrane (Invitrogen) and incubated with 1:1000 dilution of a rabbit anti-cofilin antibody (Cell Signaling), followed by incubation with 1: 1000 dilution of a goat anti-rabbit antibody conjugated with horseradish preoxidase (KPL). Signals were acquired by using SuperSignal West Femto Maximum Sensitivity Substrate (Pierce) and a CCD camera (FluorChem 9900 Imaging Systems) (Alpha Innotech). Images were analyzed and quantified using NIH-Image Version 1.63 as suggested by the software developer.

In vitro LIMK Kinase Assay

LIMK1 kinase assay was performed using purified LIMK1 and GST-tagged recombinant human cofilin (Upstate Biotechnologies) according to the manufacturer's recommendation with minor modifications. Briefly, recombinant cofilin was incubated in 1 X Kinase reaction buffer (800 nM MOPS-NaOH, pH7.0, 200 μM EDTA) in the presence or absence of staurosporine (200 nM) or the S3, S3D, Q104 peptides. LIMK1 was serially diluted in dilution buffer (20 mM MOPS-NaOH pH 7.0, 1 mM EDTA, 0.01% Brij-35, 5% glycerol, 0.1% 2-mercaptoethanol, 1 mg/ml BSA), and then added into the reaction along with the ATP buffer (10 mM magnesium acetate, 100 μM ATP). The reaction was incubated for 15 minutes at 30ºC with constant agitation. The reaction was stopped by adding 25% (V/V) of 4 X LDS sample buffer for SDS-PAGE and heated for 10 minutes at 70ºC. Cofilin phosphorylation was analyzed by SDS-PAGE and Western blotting using a rabbi anti-phospho-cofilin (ser3) antibody (Cell Signaling) as described elsewhere.

IL-2 ELISA

IL-2 released into the cell culture supernatant was detected by a human IL-2 ELISA development kit (PeproTech) according to the manufacturer's instruction. Briefly, each well of a plate was coated with 100 μl of capture antibody (1 μg/ml), incubated overnight at room temperature, and then washed and blocked with 300 μl of blocking solution for 1 hour at room temperature. Samples in plates were incubated for 1 hour at 37ºC, and then washed and incubated with 100 μl of detection antibody (0.5 μg/ml) for 1 hour at 37ºC. Plates were washed and incubated with 100 μl of the avidin-peroxidase conjugate (1:2000 dilution) for 30 minutes at room temperature followed by washing and incubation with 100 μl of tetramethylbenzidine (TMB) substrate buffer. Plates were kinetically read using an ELx808 automatic microplate reader (Bio-Tek Instruments) at 630 nm.

ShRNA Knockdown of Cofilin in Primary Human CD4 T Cells.

Plasmids (pLOK.1-puro) carrying cofilin shRNAs (cofilin713, cofilin712, cofilin711, cofilin710, cofilin709) and a non-targeting shRNA (NTC) were purchased from Sigma. Additionally, the same plasmid containing the green fluorescent protein (GFP), Turbo GFP (Sigma), was used as a control for measuring the transduction efficiency of the shRNA vectors. Viral particles were generated by cotransfection of these plasmids with a packaging plasmid and a VSV-G envelope plasmid into HEK293T cells as suggested by the manufacturer. Viral particles were harvested and concentrated approximately 40-fold. Viral titer was estimated based on the p24 content using the Turbo GFP vector as a reference. Tubo GFP particles were directly measured by counting the GFP positive cells following transduction for 48 hours. For transduction of primary human CD4 T cells, resting cells were pre-stimulated with anti-CD3/CD28 beads (1-2 beads/cell) for 12 hours, then transduced with the cofilin shRNA or the NTC shRNA viral particles (m.o.i 0.5 to 1). Following transduction at 12 to 24 hours, beads were removed by gentle pipetting in medium and separation on a magnet.

Cells were returned to resting and continuously cultured in fresh medium containing 1 μg/ml Puromycin for 1 to 2 days. Cell debris were removed by centrifugation (500 x g) in lymphocytes separation medium (Mediatech) for 20 minutes at room temperature. Cells were washed twice with medium, counted and resuspended into fresh medium at a density of 1 million per milliliter in 5ml Polypropylene Falcon round bottom tubes (BD Biosciences). Cells were rested for 6-12 hours, analyzed for the phenotype by F-actin staining, and then infected with HIV-1.

Supplemental References

Adachi, A., Gendelman, H. E., Koenig, S., Folks, T., Willey, R., Rabson, A., and Martin, M. A. (1986). Production of acquired immunodeficiency syndrome-associated retrovirus in human and nonhuman cells transfected with an infectious molecular clone. J. Virol. *59*, 284-291.

Aizawa, H., Sutoh, K., Tsubuki, S., Kawashima, S., Ishii, A., and Yahara, I. (1995). Identification, characterization, and intracellular distribution of cofilin in Dictyostelium discoideum. J. Biol. Chem. *270*, 10923-10932.

Alkhatib, G., Locati, M., Kennedy, P. E., Murphy, P. M., and Berger, E. A. (1997). HIV-1 coreceptor activity of CCR5 and its inhibition by chemokines: independence from G protein signaling and importance of coreceptor downmodulation. Virology *234*, 340-348.

Arai, H., and Charo, I. F. (1996). Differential regulation of G-protein-mediated signaling by chemokine receptors. J. Biol. Chem. *271*, 21814-21819.

Aramori, I., Ferguson, S. S., Bieniasz, P. D., Zhang, J., Cullen, B., and Cullen, M. G. (1997). Molecular mechanism of desensitization of the chemokine receptor CCR-5: receptor signaling and internalization are dissociable from its role as an HIV-1 co-receptor. Embo J. *16*, 4606-4616.

Brelot, A., Heveker, N., Montes, M., and Alizon, M. (2000). Identification of residues of CXCR4 critical for human immunodeficiency virus coreceptor and chemokine receptor activities. J. Biol. Chem. *275*, 23736-23744.

Bubb, M. R., Spector, I., Beyer, B. B., and Fosen, K. M. (2000). Effects of jasplakinolide on the kinetics of actin polymerization. An explanation for certain in vivo observations. J. Biol. Chem. *275*, 5163-5170.

Campbell, E. M., Nunez, R., and Hope, T. J. (2004). Disruption of the actin cytoskeleton can complement the ability of Nef to enhance human immunodeficiency virus type 1 infectivity. J. Virol. *78*, 5745-5755.

Cavrois, M., De Noronha, C., and Greene, W. C. (2002). A sensitive and specific enzyme-based assay detecting HIV-1 virion fusion in primary T lymphocytes. Nat. Biotechnol. *20*, 1151-1154.

Cocchi, F., DeVico, A. L., Garzino-Demo, A., Cara, A., Gallo, R. C., and Lusso, P. (1996). The V3 domain of the HIV-1 gp120 envelope glycoprotein is critical for chemokine-mediated blockade of infection. Nat. Med. *2*, 1244-1247.

Coue, M., Brenner, S. L., Spector, I., and Korn, E. D. (1987). Inhibition of actin polymerization by latrunculin A. FEBS Lett. *213*, 316-318.

Dalgleish, A. G., Beverley, P. C., Clapham, P. R., Crawford, D. H., Greaves, M. F., and Weiss, R. A. (1984). The CD4 (T4) antigen is an essential component of the receptor for the AIDS retrovirus. Nature *312*, 763-767.

Doranz, B. J., Orsini, M. J., Turner, J. D., Hoffman, T. L., Berson, J. F., Hoxie, J. A., Peiper, S. C., Brass, L. F., and Doms, R. W. (1999). Identification of CXCR4 domains that support coreceptor and chemokine receptor functions. J. Virol. *73*, 2752-2761.

Ducrey-Rundquist, O., Guyader, M., and Trono, D. (2002). Modalities of interleukin-7-induced human immunodeficiency virus permissiveness in quiescent T lymphocytes. J. Virol. *76*, 9103-9111.

Dustin, M. L., and Springer, T. A. (1989). T-cell receptor cross-linking transiently stimulates adhesiveness through LFA-1. Nature *341*, 619-624.

Endres, M. J., Clapham, P. R., Marsh, M., Ahuja, M., Turner, J. D., McKnight, A., Thomas, J. F., Stoebenau-Haggarty, B., Choe, S., Vance, P. J.*, et al.* (1996). CD4-independent infection by HIV-2 is mediated by fusin/CXCR4. Cell *87*, 745-756.

Faltynek, C. R., Schroeder, J., Mauvais, P., Miller, D., Wang, S., Murphy, D., Lehr, R., Kelley, M., Maycock, A., Michne, W., and et al. (1995). Damnacanthal is a highly potent, selective inhibitor of p56lck tyrosine kinase activity. Biochemistry *34*, 12404-12410.

Farzan, M., Choe, H., Martin, K. A., Sun, Y., Sidelko, M., Mackay, C. R., Gerard, N. P., Sodroski, J., and Gerard, C. (1997). HIV-1 entry and macrophage inflammatory protein-1beta-mediated signaling are independent functions of the chemokine receptor CCR5. J. Biol. Chem. *272*, 6854-6857.

Freed, E. O., Delwart, E. L., Buchschacher, G. L., Jr., and Panganiban, A. T. (1992). A mutation in the human immunodeficiency virus type 1 transmembrane glycoprotein gp41 dominantly interferes with fusion and infectivity. Proc. Natl. Acad. Sci. U S A *89*, 70-74.

Gerlach, L. O., Skerlj, R. T., Bridger, G. J., and Schwartz, T. W. (2001). Molecular interactions of cyclam and bicyclam non-peptide antagonists with the CXCR4 chemokine receptor. J. Biol. Chem. *276*, 14153-14160.

Gosling, J., Monteclaro, F. S., Atchison, R. E., Arai, H., Tsou, C. L., Goldsmith, M. A., and Charo, I. F. (1997). Molecular uncoupling of C-C chemokine receptor 5-induced chemotaxis and signal transduction from HIV-1 coreceptor activity. Proc. Natl. Acad. Sci. U S A *94*, 5061-5066.

Hesselgesser, J., Liang, M., Hoxie, J., Greenberg, M., Brass, L. F., Orsini, M. J., Taub, D., and Horuk, R. (1998). Identification and characterization of the CXCR4 chemokine receptor in human T cell lines: ligand binding, biological activity, and HIV-1 infectivity. J. Immunol *160*, 877-883.

Hotulainen, P., Paunola, E., Vartiainen, M. K., and Lappalainen, P. (2005). Actin-depolymerizing factor and cofilin-1 play overlapping roles in promoting rapid F-actin depolymerization in mammalian nonmuscle cells. Mol Biol Cell *16*, 649-664.

Iyengar, S., Hildreth, J. E., and Schwartz, D. H. (1998). Actin-dependent receptor colocalization required for human immunodeficiency virus entry into host cells. J. Virol *72*, 5251-5255.

Kreisberg, J. F., Yonemoto, W., and Greene, W. C. (2006). Endogenous factors enhance HIV infection of tissue naive CD4 T cells by stimulating high molecular mass APOBEC3G complex formation. J. Exp. Med. *203*, 865-870.

Kubbies, M., Goller, B., Russmann, E., Stockinger, H., and Scheuer, W. (1989). Complex Ca2+ flux inhibition as primary mechanism of staurosporine-induced impairment of T cell activation. Eur. J. Immunol. *19*, 1393-1398.

Lassen, K. G., Ramyar, K. X., Bailey, J. R., Zhou, Y., and Siliciano, R. F. (2006). Nuclear retention of multiply spliced HIV-1 RNA in resting CD4+ T cells. PLoS Pathog *2*, e68.

Lu, Z., Berson, J. F., Chen, Y., Turner, J. D., Zhang, T., Sharron, M., Jenks, M. H., Wang, Z., Kim, J., Rucker, J.*, et al.* (1997). Evolution of HIV-1 coreceptor usage through interactions with distinct CCR5 and CXCR4 domains. Proc. Natl. Acad. Sci. U S A *94*, 6426-6431.

McManus, M. T., Haines, B. B., Dillon, C. P., Whitehurst, C. E., van Parijs, L., Chen, J., and Sharp, P. A. (2002). Small interfering RNA-mediated gene silencing in T lymphocytes. J. Immunol *169*, 5754-5760.

Morton, W. M., Ayscough, K. R., and McLaughlin, P. J. (2000). Latrunculin alters the actin-monomer subunit interface to prevent polymerization. Nat. Cell. Biol. *2*, 376-378.

Mouneimne, G., Soon, L., DesMarais, V., Sidani, M., Song, X., Yip, S. C., Ghosh, M., Eddy, R., Backer, J. M., and Condeelis, J. (2004). Phospholipase C and cofilin are required for carcinoma cell directionality in response to EGF stimulation. J. Cell. Biol. *166*, 697-708.

Nebl, G., Fischer, S., Penzel, R., and Samstag, Y. (2004). Dephosphorylation of cofilin is regulated through Ras and requires the combined activities of the Ras-effectors MEK and PI3K. Cell Signal. *16*, 235-243.

O'Doherty, U., Swiggard, W. J., Jeyakumar, D., McGain, D., and Malim, M. H. (2002). A sensitive, quantitative assay for human immunodeficiency virus type 1 integration. J. Virol. *76*, 10942-10950.

O'Farrell, P. Z., Goodman, H. M., and O'Farrell, P. H. (1977). High resolution two-dimensional electrophoresis of basic as well as acidic proteins. Cell *12*, 1133-1141.

Peters, J. D., Furlong, M. T., Asai, D. J., Harrison, M. L., and Geahlen, R. L. (1996). Syk, activated by cross-linking the B-cell antigen receptor, localizes to the cytosol where it interacts with and phosphorylates alpha-tubulin on tyrosine. J. Biol. Chem. *271*, 4755-4762.

Pierson, T. C., Zhou, Y., Kieffer, T. L., Ruff, C. T., Buck, C., and Siliciano, R. F. (2002). Molecular characterization of preintegration latency in human immunodeficiency virus type 1 infection. J. Virol. *76*, 8518-8531.

Pontow, S. E., Heyden, N. V., Wei, S., and Ratner, L. (2004). Actin cytoskeletal reorganizations and coreceptor-mediated activation of rac during human immunodeficiency virus-induced cell fusion. J. Virol. *78*, 7138-7147.

Schols, D., Struyf, S., Van Damme, J., Este, J. A., Henson, G., and De Clercq, E. (1997). Inhibition of T-tropic HIV strains by selective antagonization of the chemokine receptor CXCR4. J. Exp. Med. *186*, 1383-1388.

Schrager, J. A., and Marsh, J. W. (1999). HIV-1 Nef increases T cell activation in a stimulus-dependent manner. Proc. Natl. Acad. Sci. U S A *96*, 8167-8172.

Shugars, D. C., Smith, M. S., Glueck, D. H., Nantermet, P. V., Seillier-Moiseiwitsch, F., and Swanstrom, R. (1993). Analysis of human immunodeficiency virus type 1 nef gene sequences present in vivo. J. Virol. *67*, 4639-4650.

Sidani, M., Wessels, D., Mouneimne, G., Ghosh, M., Goswami, S., Sarmiento, C., Wang, W., Kuhl, S., El-Sibai, M., Backer, J. M.*, et al.* (2007). Cofilin determines the migration behavior and turning frequency of metastatic cancer cells. J. Cell Biol. *179*, 777-791.

Simon, M. I., Strathmann, M. P., and Gautam, N. (1991). Diversity of G proteins in signal transduction. Science *252*, 802-808.

Spector, I., Shochet, N. R., Kashman, Y., and Groweiss, A. (1983). Latrunculins: novel marine toxins that disrupt microfilament organization in cultured cells. Science *219*, 493-495.

Su, S. B., Gong, W., Grimm, M., Utsunomiya, I., Sargeant, R., Oppenheim, J. J., and Ming Wang, J. (1999). Inhibition of tyrosine kinase activation blocks the down-regulation of CXC chemokine receptor 4 by HIV-1 gp120 in CD4+ T cells. J. Immun. *162*, 7128-7132.

Tamaoki, T., Nomoto, H., Takahashi, I., Kato, Y., Morimoto, M., and Tomita, F. (1986). Staurosporine, a potent inhibitor of phospholipid/Ca++dependent protein kinase. Biochem. Biophys. Res. Commun. *135*, 397-402.

Unutmaz, D., KewalRamani, V. N., Marmon, S., and Littman, D. R. (1999). Cytokine signals are sufficient for HIV-1 infection of resting human T lymphocytes. J. Exp. Med. *189*, 1735-1746.

Wu, Y., Beddall, M. H., and Marsh, J. W. (2007a). Rev-dependent indicator T cell line. Curr. HIV Rese. *5*, 395-403.

Wu, Y., Beddall, M. H., and Marsh, J. W. (2007b). Rev-dependent lentiviral expression vector. Retrovirology *4*, 12.

Wu, Y., and Marsh, J. W. (2001). Selective transcription and modulation of resting T cell activity by preintegrated HIV DNA. Science *293*, 1503-1506.

Wu, Y., and Marsh, J. W. (2003). Early transcription from nonintegrated DNA in human immunodeficiency virus infection. J. Virol. *77*, 10376-10382.

Wulfing, C., and Davis, M. M. (1998). A receptor/cytoskeletal movement triggered by costimulation during T cell activation. Science *282*, 2266-2269.

Young, I. T. (1977). Proof without prejudice: use of the Kolmogorov-Smirnov test for the analysis of histograms from flow systems and other sources. J. Histochem. Cytochem. *25*, 935-941.

Zaitseva, M., Romantseva, T., Manischewitz, J., Wang, J., Goucher, D., and Golding, H. (2005). Increased CXCR4-dependent HIV-1 fusion in activated T cells: role of CD4/CXCR4 association. J. Leukoc. Biol. *78*, 1306-1317.